JOURNAL OF PETROLOGY | VOLUME 44 | NUMBER 2 | PAGES 279–304 | 2003

The Prinsen af Wales Bjerge Formation Lavas, East Greenland: the Transition from Tholeiitic to Alkalic Magmatism during Palaeogene Continental Break-up

D. W. PEATE[1]*, J. A. BAKER[1], J. BLICHERT-TOFT[2], D. R. HILTON[3], M. STOREY[1], A. J. R. KENT[1]†, C. K. BROOKS[1,4], H. HANSEN[1]‡, A. K. PEDERSEN[1,5] AND R. A. DUNCAN[6]

[1]DANISH LITHOSPHERE CENTRE, ØSTER VOLDGADE 10-L, DK-1350 COPENHAGEN K, DENMARK

[2]LABORATOIRE DES SCIENCES DE LA TERRE, ÉCOLE NORMALE SUPÉRIEURE DE LYON, 46 ALLÉE D'ITALIE, 69364 LYON CEDEX 7, FRANCE

[3]GEOSCIENCES RESEARCH DIVISION, SCRIPPS INSTITUTION OF OCEANOGRAPHY, LA JOLLA, CA 92093-0220, USA

[4]GEOLOGICAL INSTITUTE, UNIVERSITY OF COPENHAGEN, ØSTER VOLDGADE 10-L, DK-1350 COPENHAGEN K, DENMARK

[5]GEOLOGICAL MUSEUM, ØSTER VOLDGADE 5, DK-1350 COPENHAGEN K, DENMARK

[6]COLLEGE OF OCEANIC AND ATMOSPHERIC SCIENCES, OREGON STATE UNIVERSITY, CORVALLIS, OR 97331, USA

RECEIVED NOVEMBER 1, 2001; REVISED TYPESCRIPT ACCEPTED AUGUST 8, 2002

We present elemental and isotopic (Sr–Nd–Pb–Hf–Os–He) data on primitive alkalic lavas from the Prinsen af Wales Bjerge, East Greenland. Stratigraphical, compositional and ^{40}Ar–^{39}Ar data indicate that this inland alkalic activity was contemporaneous with the upper parts of the main tholeiitic plateau basalts and also post-dated them. The alkalic rocks show a marked crustal influence, indicating establishment of new magmatic plumbing systems distinct from the long-lived coastal systems that fed the relatively uncontaminated plateau basalts. The least contaminated lavas have high $^{3}He/^{4}He$ isotope ratios (R/R_A 12·4–18·5), sub-chondritic $^{187}Os/^{188}Os_i$ (0·120–0·126), low εNd_i ($\sim +4$) and εHf_i ($\sim +6$) that plot below the 'Nd–Hf mantle array', and trace element characteristics similar to HIMU ocean island basalt (OIB). The uncontaminated magma is inferred to have more radiogenic $^{206}Pb/^{204}Pb$ values (>19·2) than the plateau basalts and Icelandic basalts, and thus represents a possible 'enriched' component to explain the compositional variations within the plateau basalts. One model to explain these compositional features is preferential melting of recycled material within the plume upwelling beneath the thick lithospheric cap, with ^{3}He contributed from volatile-rich fluids from elsewhere in the Icelandic plume. The exact nature of the recycled component is not yet resolved, although Hf isotope compositions rule out any significant role for recycled pelagic sediment, and the low $^{187}Os/^{188}Os$ limits the participation of recycled basaltic material and argues instead for a contribution from the mantle section of the recycled slab.

KEY WORDS: *alkalic lavas; flood basalts; high $^{3}He/^{4}He$; East Greenland; recycled lithosphere; Iceland plume*

INTRODUCTION

The extensive Early Palaeogene tholeiitic magmatism on the margins of Greenland and NW Europe, which

*Corresponding author. Telephone: (+45) 38 14 2664. Fax: (+45) 38 10 0878. E-mail: dwp@dlc.ku.dk

†Present address: Department of Geosciences, Oregon State University, Corvallis, OR 97331-5506, USA.

‡Present address: Geological Survey of Greenland and Denmark, Øster Voldgade 10, DK-1350, Copenhagen K, Denmark.

comprise the North Atlantic Igneous Province, is generally attributed to mantle decompression melting, driven both by the arrival of the Iceland mantle plume and the subsequent rifting that led to continental break-up and the opening of the North Atlantic Ocean (e.g. Saunders *et al.*, 1997). Volumetrically minor alkalic magmatism is found along the East Greenland coast (66–74°N), especially as highly silica-undersaturated rocks that occur mainly as intrusive complexes, but with some lavas and tephra (Nielsen, 1987). The possible origins of such alkalic rocks associated with tholeiitic flood basalts include low-degree melting of plume mantle beneath a thick lithospheric cap (e.g. Brown *et al.*, 1996), preferential melting of enriched components within the plume such as recycled oceanic crust (e.g. Bernstein *et al.*, 2000), and melting of enriched material within the continental mantle lithosphere by conductive heating from the plume (e.g. Carlson *et al.*, 1996).

The most extensive sequence of alkalic lavas is in the inland Prinsen af Wales Bjerge (Fig. 1), where they form a series of small volcanic centres overlying the main tholeiitic plateau basalts (Wager, 1947; Brown *et al.*, 1996; Hansen *et al.*, 2002). Four stratigraphic profiles were sampled through lava sequences in the northern Prinsen af Wales Bjerge by parties from the Danish Lithosphere Centre. We present new elemental and isotopic (Sr–Nd–Pb–Hf–Os–He) data on these samples to investigate the relationship between the alkalic lavas and the underlying tholeiitic flood basalts. In addition, we address the nature of the mantle sources involved during the waning stages of magmatism that accompanied continental break-up in the North Atlantic region.

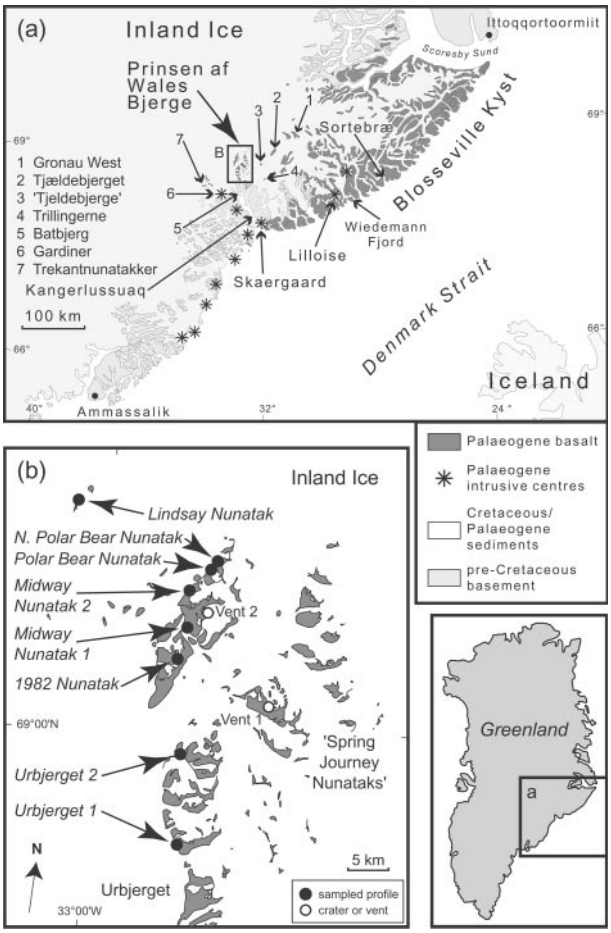

Fig. 1. (a) Location map of the East Greenland flood basalts and their relationship to the Iceland plume. Place names enclosed in inverted commas are informal names in regular use that are not yet officially recognized. It should be noted that the nunataks officially referred to as Tjældbjerget (2 on map) are not the same location that Wager (1947) called 'Tjeldebjerge' (3 on map). (b) Map of the Prinsen af Wales Bjerge region showing the locations of the studied sections (informal profile names in italics). Details of the Urbjerget 1 and 2 and 1982 Nunatak profiles have been given by Hansen *et al.* (2002). Vent 1 is the location of sample 436231, which gives an ^{40}Ar–^{39}Ar age of 53 Ma, and vent 2 has been described by Hansen *et al.* (2002).

GEOLOGICAL BACKGROUND TO THE PRINSEN AF WALES BJERGE LAVAS

East Greenland flood basalt succession

The main Palaeogene lava sequences in East Greenland are in the Blosseville Kyst region (Fig. 1a). The lava stratigraphy of the coastal region is well established, and most of these tholeiitic lavas were erupted in two distinct phases (Storey *et al.*, 1996) comparable with the main magmatic episodes recognized throughout the North Atlantic Igneous Province (Saunders *et al.*, 1997): (1) the earliest volcanic rocks that include the Lower Basalts (Nielsen *et al.*, 1981) at 61–57 Ma, followed by (2) the eruption at 56–54 Ma of the voluminous plateau basalts. The main phase of flood volcanism is divided into four stratigraphic formations (from base to top: Milne Land, Geikie Plateau, Rømer Fjord, and Skrænterne), based on field appearance, petrography, and composition (Larsen *et al.*, 1989; Pedersen *et al.*, 1997). The term 'plateau basalt(s)' is used here as a collective term for these four formations (after Hansen *et al.*, 2002). A younger magmatic phase (50–47 Ma) is represented by volumetrically minor Igtertivâ Formation lavas that cap the plateau basalts in the NE of the Blosseville Kyst region (Larsen *et al.*, 1989), by some mafic intrusions along the coast (Tegner *et al.*, 1998*a*), and by some offshore lavas (Tegner & Duncan, 1999). A tectonic model to account for these discrete mantle melting episodes has been proposed by Saunders *et al.* (1997) and Tegner *et al.* (1998*a*). The initial phase is inferred to represent the initial impact and rapid dispersal of Iceland plume-head material over a broad area in the shallow upper mantle, resulting in synchronous initiation of magmatism from

Baffin Island to Scotland. The driving force behind the second phase of activity is likely to have been decompression melting accompanying the initial plate break-up and opening of the North Atlantic Ocean. Tegner *et al.* (1998*a*) interpreted the third phase as resulting from the passage of the Iceland plume stem beneath the East Greenland rifted margin, although hotspot track reconstructions (Lawver & Müller, 1994; Torsvik *et al.*, 2001) suggest that the plume axis was beneath the thick Greenland craton, ~300 km inland at this time.

The Prinsen af Wales Bjerge region and sampled profiles

The inland lavas north of Kangerlussuaq (Fig. 1) have rarely been visited. Previous expeditions to the Prinsen af Wales Bjerge region in 1935–1936 (Wager, 1947; Anwar, 1955; Fawcett *et al.*, 1982; Noble *et al.*, 1988; Brown *et al.*, 1996, 2000) and 1982 (Hogg, 1985; Hogg *et al.*, 1989; Hansen *et al.*, 2002) found alkalic lavas with variable dips, overlying a series of flat-lying tholeiitic lavas. This was interpreted as a series of late-stage alkalic shield volcanoes that developed as the main plateau basalt eruptions came to an end. Published K–Ar ages for Prinsen af Wales Bjerge lavas lie in the range 51–60 Ma (Noble *et al.*, 1988). Hansen *et al.* (2002) developed a regional stratigraphy for this inland area, based on photogrammetry, new sampled profiles (Fig. 1b), and a compilation of existing and new compositional data. Parts of these sequences can be correlated with the existing coastal stratigraphy (Pedersen *et al.*, 1997), but some compositional units are not found at the coast. In the Urbjerget profiles, there are a few lavas, lying on basement gneisses, that are correlated stratigraphically with the coastal Lower Basalts, and dated by ^{40}Ar–^{39}Ar at ~61 Ma (Hansen *et al.*, 2002). These are overlain by a younger sequence of high-Ti picrites, unknown elsewhere along the Blosseville coast, and then by tholeiitic basalts inferred to be part of the Milne Land Formation, the lowermost part of the plateau basalts (Hansen *et al.*, 2002). In the northern Prinsen af Wales Bjerge profiles, tholeiitic basalts are interbedded with, and overlain by, a series of alkalic lavas. These alkalic lavas have generally been referred to as the Prinsen af Wales basalts, but Hansen *et al.* (2002) formalized them as the Prinsen af Wales Bjerge Formation. Compositional data on the lower parts of this inland lava sequence as well as alkalic lavas from 1982 Nunatak (Fig. 1) have been given by Hansen *et al.* (2002). Here, we focus on the upper parts, to evaluate the origin of the alkalic basalts that make up the Prinsen af Wales Bjerge Formation, and their relationship to the underlying tholeiitic plateau basalts.

Multi-model photogrammetric analysis using stereo photographs obtained in 1994 (Pedersen *et al.*, 1997; Hansen *et al.*, 2002) was used to select four stratigraphic profiles for detailed flow-by-flow sampling during expeditions in 1995 and 2000. Profile locations and stratigraphic details are shown in Figs 1b and 2, respectively. Reconnaissance sampling in 1995 of 'Lindsay Nunatak' to the NW of the Prinsen af Wales Bjerge (Fig. 1) found younger, tholeiitic picrites above the alkalic lavas. We also present major element data on dykes from the southern part of the Prinsen af Wales Bjerge and from areas farther south to demonstrate their compositional similarity to the Prinsen af Wales Bjerge alkalic lavas, attesting to the widespread distribution of this compositional type: one dyke from the Urbjerget 2 section (Fig. 1b: Hansen *et al.*, 2002), and five dykes collected in 1975 that cross-cut the ~445 Ma Batbjerg intrusion (Fig. 1a: Brooks *et al.*, 1976; Fawcett *et al.*, 1982).

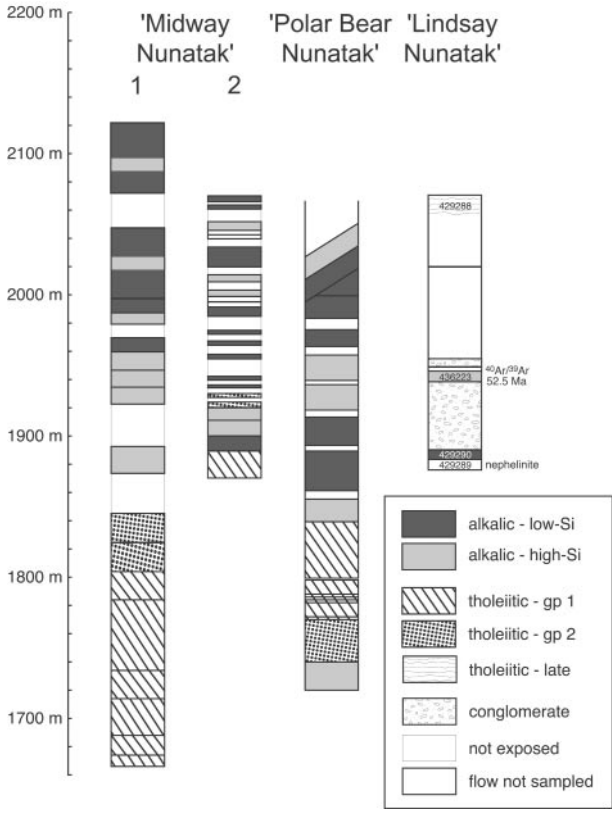

Fig. 2. Stratigraphic profiles sampled in the northern Prinsen af Wales Bjerge and 'Lindsay Nunatak'. Altitudes are approximate, based on using field altimeters plus some independent constraint from subsequent photogrammetry. The sample collection analysed from 'Lindsay Nunatak' came from a short reconnaissance visit in 1995, and their approximate stratigraphic locations have been estimated based on a more comprehensive profile made in 2000. Sample 429291 is from a loose block and either is a clast within the upper conglomerate or comes from one of the flow units that overlie the upper conglomerate unit. The lower conglomerate contains many clasts that are petrographically similar to samples from the nearby Gardiner Intrusion that has been dated at 56–54 Ma (Waight *et al.*, 2002*b*).

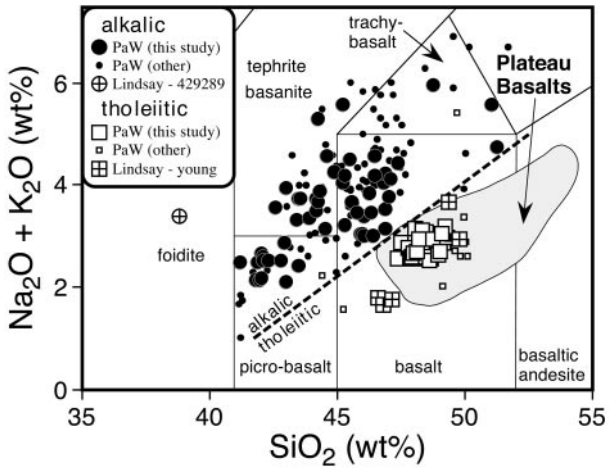

Fig. 3. Total alkalis–silica classification diagram (Le Bas, 2000). All of the alkalic lavas that fall within the picro-basalt field are, in fact, picrites according to revised definitions of Le Bas (2000), with the exception of one of the Batbjerg dykes. The division between alkalic and tholeiite lavas is from MacDonald & Katsura (1964). Published analyses from Prinsen af Wales Bjerge and Trekantnunatakker alkalic and tholeiitic lavas are labelled as 'other' (Hogg, 1985; Hogg *et al.*, 1989; Brown *et al.*, 1996, 2000; Hansen *et al.*, 2002); field for coastal plateau basalts from Scoresby Sund (Larsen *et al.*, 1989). Highly altered samples with 'volatiles' (see Table 3 caption) >4 wt % are not plotted.

Table 1: $^{40}Ar/^{39}Ar$ age data for two Prinsen af Wales Bjerge Formation samples

Step	Temp. (°C)	Age (Ma)	2σ	% $^{40}Ar_R$	% total ^{39}Ar
Sample 436231, plagioclase					
1	800	54·9	0·3	93·27	57·8
2	850	54·4	0·9	94·97	19·1
3	900	54·8	1·2	81·92	4·9
4	1000	55·3	2·1	76·91	4·7
5	1125	53·6	1·8	84·90	5·9
6	1325	54·3	1·2	83·70	7·6
Sample 436223, whole rock					
1	600	55·5	2·56	18·12	4·85
2	800	53·9	1·54	53·82	10·48
3	900	53·67	1·15	37·36	18·07
4	1000	52·7	0·56	71·26	28·51
5	1250	50·75	0·69	74·25	22·01
6	fusion	49·71	0·93	81·78	16·1

Plagioclase sample 436231 is from a pegmatite from vent 1 (see Fig. 1). It was heated using a Heine, low-blank, double vacuum furnace, and the argon isotopic composition was analysed on a MAP 215-50 mass spectrometer. For this sample, plateau age (steps 1–6; 100% ^{39}Ar released) = **54·88 ± 0·97 Ma**; inverse isochron (steps 1–6) = **55·07 ± 1·08 Ma**; $^{40}Ar/^{36}Ar_i$ = 284·4 ± 28·6; J = 0·0016533 ± 0·0000142. Whole-rock sample 436223 is from a lava from 'Lindsay Nunatak' (see Fig. 1). It was heated inductively using a radio-frequency induced heating coil and analysed on an AEI MS-10S mass spectrometer. For this sample, plateau age (steps 1–4; 61·9% ^{39}Ar released) = **53·08 ± 1·17 Ma**; inverse isochron (steps 1–4) = **52·52 ± 1·10 Ma**; $^{40}Ar/^{36}Ar_i$ = 299·4 ± 3·1; J = 0·0014500 ± 0·0000135. All calculations are relative to monitor FCT-3 biotite (28·04 ± 0·12 Ma). All errors are 2σ. [See Storey *et al.* (1998) for further details.]

RESULTS

Sample classification and petrography

Using the IUGS classification scheme (Le Bas, 2000), most samples classify as picrites, basalts, trachybasalts and basanites. The total alkalis vs silica diagram (Fig. 3) shows the clear division of the analysed samples into alkalic and tholeiitic magmas, using the alkalic–tholeiitic boundary from Hawaii (MacDonald & Katsura, 1964). The tholeiitic lavas are found at the base of the sampled profiles, and overlap with the field for the coastal plateau basalts. The uppermost, tholeiitic flows at 'Lindsay Nunatak' are an exception as they overlie alkalic lavas that are younger than the plateau basalts based on new ^{40}Ar–^{39}Ar dating (see below). The alkalic lavas are mildly alkalic, with CIPW norm calculations indicating that just over half are nepheline normative. The lowermost flow at 'Lindsay Nunatak' (429289) is nepheline normative but different from the other alkalic rocks as it has lower SiO_2 and thus classifies as a nephelinite.

Detailed petrographic descriptions of the Prinsen af Wales Bjerge lavas have been given by Anwar (1955), Hogg (1985) and Brown *et al.* (1996, 2000). The tholeiitic lavas are virtually aphyric (<5% plagioclase phenocrysts), except for two samples (429246 and 429250) that have up to 15% plagioclase phenocrysts, and the uppermost flow at 'Lindsay Nunatak' that is olivine-phyric (429288: ~30% 1–2 mm euhedral olivine phenocrysts). Most alkalic samples are porphyritic, with up to 40% sub- to euhedral phenocrysts (2–10 mm) of olivine and/or clinopyroxene, although a few are virtually aphyric. Although our samples are mainly picritic (olivine-dominated, with <5% clinopyroxene phenocrysts), Brown *et al.* (1996, 2000) documented some ankaramitic (clinopyroxene-dominated) flows from other localities.

^{40}Ar–^{39}Ar geochronology

Two alkalic lava samples were selected for dating by the step-heating ^{40}Ar–^{39}Ar method. The data are presented in Table 1 [see table legend and Storey *et al.* (1998) for analytical details]. Sample 436223 is a lava from the middle of the 'Lindsay Nunatak' profile (Fig. 2), and a whole-rock sample gave a plateau age of 52·5 ± 0·3 Ma

(Table 1). The isochron age for this sample is concordant with the plateau age and the initial $^{40}Ar/^{36}Ar$ ratio is within error of the atmospheric value. Sample 436231 is an evolved, pegmatitic sample from a vent site in the Spring Journey Nunataks (vent 1, Fig. 1). A plagioclase separate gave a plateau age of 54·9 ± 1·0 Ma and a concordant isochron age of 55·1 ± 1·1 Ma with an atmospheric initial $^{40}Ar/^{36}Ar$ ratio. The age for sample 436223 confirms inferences from field relations that parts of the Prinsen af Wales Bjerge Formation magmatism postdate the eruption of the coastal plateau basalts (56–54 Ma: Storey *et al.*, 1996). However, the older age for sample 436231 provides the first indication that some of this alkalic magmatism was contemporaneous with the plateau basalt eruptions.

Major element variations

Major element data on 77 samples, analysed by X-ray fluorescence spectrometry, are given in Table 2. The variations of selected major elements with MgO, an index of crystal fractionation, are shown in Fig. 4. Some samples have elevated 'volatiles' values (see table legend) consistent with petrographic evidence for post-eruptive alteration and weathering. However, these make up only a small proportion of the analysed samples (only 12 out of 77 analysed samples have 'volatiles' values >2·5 wt % and most of these are dykes). Although alteration affects most samples to some extent (e.g. the greater data scatter in Fig. 4 of K_2O, a fluid-mobile element, compared with TiO_2), we believe that our overall petrogenetic conclusions are robust as they are based in general on variations of the more immobile elements in the freshest-looking samples.

The main tholeiitic lavas have a restricted compositional range (MgO 6·0–7·2 wt %) and lower TiO_2, relative to the alkalic lavas (MgO 4–25 wt %). The youngest tholeiitic flow (429288) at 'Lindsay Nunatak' has high MgO (~20 wt %), and some other highly magnesian tholeiites have been reported from Trekantnunatakker and 'Tjeldebjerge' (Brown *et al.*, 1996, 2000). The main tholeiitic lavas show a significant range in TiO_2 for a given MgO content, indicating that the samples cannot simply be related to a common parental magma by different extents of fractional crystallization. Two distinct subgroups can be recognized: Group 1 have TiO_2 <3·2 wt % and SiO_2 >48·2 wt %, whereas Group 2 have TiO_2 >3·2 wt % and SiO_2 <48·2 wt %. Two samples (429246 and 429250) have anomalously high Al_2O_3 indicative of plagioclase accumulation, which is consistent with their plagioclase-phyric petrography. The Group 1 flows dominate the tholeiitic lavas in the sampled profiles, with the Group 2 flows comprising just one or two relatively thin flows in each profile (Fig. 2).

Most of the alkalic lavas have between 7 and 20 wt % MgO, and they can be divided into two subgroups: a main group with low SiO_2 (41–45 wt %) and high TiO_2 (4·0–5·5 wt %), and an Si-enriched group with higher SiO_2 (46–51 wt %) and lower TiO_2 (2·5–4·7 wt %). The most mafic sample (429235; 25 wt % MgO) is also considered to belong to the high-Si group. The 'Lindsay Nunatak' nephelinite is distinct from the other alkalic lavas, in having very low SiO_2 (~39 wt %), low MgO (~7 wt %), and high TiO_2 (~8 wt %), although broadly similar compositions are found in dykes from the nearby Gardiner Intrusion (Fig. 1: Nielsen, 1994) and in dykes traversing the Kangerlussuaq region to the south (Brooks & Rucklidge, 1974).

For the high-MgO samples (>10 wt % MgO), major element variations are controlled by olivine fractionation or accumulation. Clinopyroxene joins the fractionating assemblage at ~10 wt % MgO, as indicated by the inflection on the CaO vs MgO diagram (Fig. 4e). Despite the high MgO contents of the alkalic lavas, their highly porphyritic nature suggests that they are unlikely to represent liquid compositions. However, Brown *et al.* (1996) found some very magnesian olivines (up to $Fo_{91·3}$) in one alkalic picrite, and commented that such olivines would be in equilibrium with a liquid similar in composition to the host bulk-rock sample, and therefore that such high-MgO (~18 wt %) magmas might have existed.

Trace element variations

Trace element data, analysed by inductively coupled plasma mass spectrometry (ICP-MS) on selected samples, are presented in Table 3. Primitive-mantle-normalized trace element patterns of representative unaltered samples are shown in Fig. 5a. The two tholeiitic compositional sub-groups, recognized from major element differences, are also distinct in terms of trace elements. The high-TiO_2 Group 2 lavas have higher incompatible element abundances and more light rare earth element (LREE) enriched patterns compared with the main low-TiO_2 Group 1 lavas (La/Yb_N 3·9–4·2 vs 3·0–3·5: where subscript N indicates chondrite normalized). The upper tholeiitic lava at 'Lindsay Nunatak' (429288) has a similar trace element pattern to the Group 2 tholeiites (La/Yb_N 4·9), except for higher Pb, Ba, Rb, K and Sr, whereas the other 'Lindsay Nunatak' tholeiite (429291) has an enriched pattern with La/Yb_N of 11, similar to some of the high-Si alkalic lavas (neither are illustrated in Fig. 5a). Similarly enriched tholeiitic lavas have been found at 1982 Nunatak (Hogg *et al.*, 1989).

The alkalic lavas have higher incompatible trace element abundances and strongly LREE-enriched patterns relative to the tholeiitic lavas (La/Yb_N 12–28 vs 3–5). The main group show relatively smooth patterns, with

Table 2: Major element and selected trace element data for lavas from the Prinsen af Wales Bjerge, East Greenland

Sample	Profile	Alt. (m)	SiO_2	TiO_2	Al_2O_3	Fe_2O_3(t)	MnO	MgO	CaO	Na_2O	K_2O	P_2O_5	Vol.	Total	Fe_2O_3	FeO	V	Cr	Ni	Cu	Zn	Sr	Zr
Alkalic lavas (Prinsen af Wales Bjerge Formation)																							
Low-Si type																							
429239	Midway 1	1965	44·83	5·23	8·50	16·29	0·19	9·55	10·52	3·06	1·19	0·64	1·64	99·65	4·82	10·19	378	463	311	200	148	774	439
429241	Midway 1	1990	42·96	5·38	7·27	15·96	0·20	12·93	10·65	2·86	1·10	0·71	2·01	99·50	4·05	10·52	370	901	445	221	144	992	473
429242	Midway 1	2010	42·94	5·41	7·34	15·97	0·20	13·00	11·52	2·06	0·81	0·73	3·00	99·32	3·92	10·49	374	889	437	178	148	1229	470
429244	Midway 1	2040	41·98	4·46	5·46	16·67	0·20	18·53	10·01	1·03	1·11	0·55	2·21	99·38	3·32	11·79	328	1162	876	203	147	1278	373
429245	Midway 1	2050	42·30	4·60	5·85	16·93	0·20	15·80	11·30	1·71	0·80	0·52	2·09	99·69	4·42	11·07	358	858	675	253	152	1499	357
429294	Midway 1	2100	42·09	5·32	6·07	17·54	0·21	13·66	11·92	1·90	0·64	0·66	2·50	99·88	2·12	14·12	398	778	542	253	171	1051	382
429295	Midway 1	2100	44·33	6·36	8·76	17·02	0·21	7·90	10·77	2·31	1·54	0·79	1·38	100·08	2·06	13·70	492	325	171	264	173	746	505
429296	Midway 1	2100	44·55	5·84	7·61	16·84	0·21	9·48	11·64	2·05	1·10	0·68	1·43	99·69	2·03	13·55	430	678	265	247	172	675	415
429297	Midway 1	2100	45·21	5·33	9·63	15·51	0·19	9·49	9·92	2·73	1·33	0·67	1·70	99·90	1·87	12·47	380	566	267	233	159	723	397
429299A	Midway 1	2100	46·44	5·00	10·93	15·10	0·19	7·46	9·96	2·66	1·53	0·73	2·82	99·54	1·82	12·13	371	316	151	140	155	949	391
429299B	Midway 1	2100	44·21	6·41	10·22	15·95	0·21	5·92	10·73	3·36	1·92	1·07	3·57	99·53	1·92	12·83	414	47	103	295	168	1294	578
458815	Midway 2	1889	43·88	3·74	7·19	14·82	0·20	16·38	9·97	1·96	1·38	0·48	1·92	99·53	4·13	9·44	273	1114	716	184	—	1053	428
458821	Midway 2	1937	44·60	5·89	10·00	17·02	0·22	7·01	9·95	2·99	1·56	0·76	2·05	99·62	7·22	8·60	400	196	177	211	—	797	624
458822	Midway 2	1940	42·03	4·25	5·68	16·35	0·20	17·99	10·32	2·03	0·63	0·52	2·18	99·82	4·77	10·24	308	1048	869	214	—	1009	465
458823	Midway 2	1955	41·88	4·17	5·33	16·59	0·20	18·63	10·24	1·88	0·60	0·48	2·06	99·69	5·80	9·51	317	1126	922	202	—	1132	451
458824	Midway 2	1964	43·57	4·02	6·86	15·41	0·19	16·12	9·60	2·70	1·04	0·48	1·89	99·54	4·56	9·58	316	1051	764	215	—	583	426
458825	Midway 2	1972	45·49	5·52	9·04	15·85	0·19	7·57	11·21	3·10	1·38	0·66	1·53	99·93	6·69	8·14	396	205	187	259	—	913	565
458826	Midway 2	1988	41·83	4·09	5·05	16·25	0·19	21·93	8·05	1·41	0·74	0·46	1·36	99·66	4·69	10·32	281	1363	1215	179	—	691	464
458829	Midway 2	2022	44·18	5·06	7·90	16·56	0·20	11·54	10·26	2·61	1·11	0·58	1·49	99·77	5·24	10·10	362	652	481	211	—	845	522
458831	Midway 2	2061	42·05	4·62	6·06	16·87	0·21	15·86	11·22	2·26	0·33	0·52	2·22	99·54	4·55	10·87	336	812	733	237	—	971	457
458832	Midway 2	2067	44·19	4·54	8·29	15·74	0·20	12·19	10·84	2·41	1·08	0·52	2·19	99·47	5·37	9·09	340	704	476	238	—	1160	451
429265	Polar Bear	1875	41·99	4·01	4·97	16·75	0·20	19·60	9·83	1·37	0·82	0·48	1·41	99·68	3·52	11·84	329	1396	925	173	148	724	325
429266	Polar Bear	1900	39·72	3·29	3·11	17·43	0·21	28·28	7·31	0·25	0·03	0·37	5·83	99·19	6·04	9·37	237	1645	1516	137	142	297	250
429269	Polar Bear	1970	45·31	4·94	7·95	16·08	0·19	10·86	10·88	2·13	1·09	0·57	1·87	99·36	4·63	10·10	386	539	374	238	145	1520	400
429270	Polar Bear	1995	45·79	4·99	8·15	15·59	0·18	9·72	11·56	2·31	1·14	0·57	1·59	99·62	4·87	9·52	393	511	300	230	142	1422	407
429271	Polar Bear	2005	45·26	5·29	8·32	15·81	0·19	9·16	11·20	3·03	1·15	0·59	2·21	99·54	8·89	5·94	402	406	225	234	141	343	411
429272	Polar Bear	2020	43·43	5·85	7·07	16·05	0·19	11·97	11·45	2·17	1·16	0·66	1·51	99·31	5·50	9·33	418	706	438	247	143	733	466
436223	Lindsay	1938	43·47	4·42	6·77	16·36	0·20	15·49	10·40	1·47	0·95	0·48	2·53	99·21	4·53	10·35	—	—	—	—	—	—	—
436231	Vent 1	—	45·21	5·12	13·99	14·65	0·19	4·18	10·21	4·00	1·56	0·89	1·94	99·57	3·36	9·99	—	—	—	—	—	—	—

Sample	Profile	Alt. (m)	SiO_2	TiO_2	Al_2O_3	Fe_2O_3(t)	MnO	MgO	CaO	Na_2O	K_2O	P_2O_5	Vol.	Total	Fe_2O_3	FeO	V	Cr	Ni	Cu	Zn	Sr	Zr
High-Si type																							
429235	Midway 1	1885	42·97	2·48	4·58	15·56	0·19	25·32	6·48	1·45	0·66	0·30	1·70	99·52	3·02	11·15	216	1513	1354	142	125	316	207
429236	Midway 1	1930	51·22	2·99	9·87	11·86	0·15	8·34	10·39	3·30	1·44	0·43	1·73	99·62	4·87	6·14	279	386	137	180	102	852	256
429237	Midway 1	1945	51·05	3·31	11·09	12·55	0·16	6·69	9·11	3·73	1·85	0·47	1·52	99·74	6·92	4·92	287	199	99	201	114	588	290
429238	Midway 1	1955	46·84	4·25	7·93	14·71	0·18	11·89	10·16	2·48	1·05	0·49	1·68	99·22	3·96	9·49	322	757	363	207	145	859	342
429240	Midway 1	1985	47·36	3·85	9·95	14·09	0·18	9·86	9·74	3·12	1·31	0·53	2·47	99·51	3·99	8·84	304	569	276	167	126	1235	328
429243	Midway 1	2025	46·77	2·50	7·81	12·59	0·16	15·99	9·72	2·88	1·17	0·41	1·61	99·62	3·04	8·47	241	873	648	185	104	1336	219
429298	Midway 1	2100	48·73	4·36	13·36	13·95	0·18	5·48	7·26	4·23	1·73	0·71	2·28	99·95	1·68	11·20	328	6	37	58	158	1191	396
458830	Midway 2	2047	46·48	2·58	8·04	12·76	0·17	15·43	9·58	3·15	1·42	0·40	1·39	99·60	2·89	8·79	232	950	642	192	—	917	311
458827	Midway 2	2000	46·27	3·47	8·14	14·75	0·19	13·23	9·70	2·77	1·09	0·40	1·53	99·92	4·16	9·46	297	821	482	190	—	1203	398
458828	Midway 2	2009	47·05	4·47	8·33	14·27	0·18	11·53	9·54	2·88	1·25	0·49	1·62	99·62	4·11	9·02	286	717	377	218	—	786	455
458816	Midway 2	1900	46·07	2·89	8·27	13·47	0·18	16·45	8·91	2·26	1·12	0·37	2·03	99·75	3·50	8·82	243	1093	751	150	—	1161	350
458818	Midway 2	1912	45·96	2·78	8·08	13·50	0·19	17·27	8·83	1·90	1·15	0·35	2·19	99·81	3·51	8·82	241	1023	779	144	—	912	358
429258	Polar Bear	1730	46·91	2·73	8·65	13·01	0·18	15·62	9·40	1·98	1·15	0·36	1·89	99·71	3·43	8·48	255	1038	627	147	115	606	225
429264	Polar Bear	1845	46·36	3·25	6·79	14·40	0·18	16·33	9·32	1·97	1·04	0·36	1·67	99·57	3·20	9·95	282	1167	695	180	125	801	267
429267	Polar Bear	1930	45·88	3·53	7·03	14·40	0·17	16·78	8·74	2·07	0·97	0·41	1·87	99·54	2·35	10·70	290	1032	776	159	124	946	286
429268	Polar Bear	1950	46·07	3·82	7·42	14·73	0·17	15·27	9·07	2·07	0·95	0·42	2·01	99·39	3·59	9·82	304	974	688	125	125	1308	298
429273	Polar Bear	2035	46·85	4·48	9·28	14·29	0·18	9·86	10·24	3·04	1·20	0·57	1·28	99·13	5·36	7·87	346	647	262	192	126	716	385
429290	Lindsay	1890	47·02	4·72	8·79	14·77	0·21	9·42	10·76	2·65	1·10	0·56	1·69	99·85	1·78	11·86	366	494	263	247	150	611	343
Nephelinite ('Lindsay Nunatak')																							
429289	Lindsay	1883	38·81	7·97	7·55	17·35	0·28	6·94	16·51	2·28	1·10	1·21	2·64	99·43	2·10	13·97	470	27	118	401	190	1495	587
Alkalic dykes (compositionally equivalent to the Prinsen af Wales Bjerge Formation lavas)																							
Low-Si type																							
429274	Polar Bear	dyke	41·21	4·31	5·18	17·22	0·20	19·48	9·38	1·68	0·81	0·54	1·38	99·26	3·80	11·95	316	1294	923	211	146	1194	350
30210	Batbjerg	dyke	42·75	6·35	8·38	17·35	0·17	8·06	13·59	1·89	0·64	0·82	3·90	99·56	5·80	9·88	—	—	—	—	—	—	—
30204	Batbjerg	dyke	45·55	5·45	9·34	15·61	0·17	7·73	11·76	2·26	1·41	0·72	3·16	100·08	7·52	6·96	—	—	—	—	—	—	—
30269	Batbjerg	dyke	43·50	5·48	7·69	15·80	0·16	11·96	11·04	2·45	1·27	0·67	3·61	100·12	3·72	10·54	—	—	—	—	—	—	—
30223	Batbjerg	dyke	42·58	5·06	6·85	15·57	0·18	16·42	9·03	2·17	1·38	0·75	2·17	100·01	4·42	9·88	—	—	—	—	—	—	—
421718	Urbjerget2	dyke	44·23	5·32	13·58	14·74	0·26	4·75	12·74	2·96	0·69	0·71	3·78	99·02	7·13	6·31	—	—	—	—	—	—	—
High-Si type																							
30213	Batbjerg	dyke	46·29	4·60	7·96	13·97	0·16	9·30	13·69	2·32	1·12	0·59	3·44	100·04	6·17	6·69	—	—	—	—	—	—	—

Table 2: continued

Sample	Profile	Alt. (m)	SiO_2	TiO_2	Al_2O_3	Fe_2O_3(t)	MnO	MgO	CaO	Na_2O	K_2O	P_2O_5	Vol.	Total	Fe_2O_3	FeO	V	Cr	Ni	Cu	Zn	Sr	Zr
Tholeiitic lavas (equivalent to plateau basalt lavas of the Blosseville Kyst)																							
'Group 1'																							
429246	Midway 1	1675	48·30	2·49	15·13	13·23	0·18	5·96	11·70	2·47	0·29	0·25	1·26	100·09	7·42	5·16	358	150	90	250	100	275	192
429247	Midway 1	1710	48·41	2·92	13·59	14·41	0·20	6·59	11·02	2·36	0·22	0·28	1·32	100·44	4·25	9·16	426	142	108	240	114	270	227
429248	Midway 1	1685	49·23	2·36	14·30	13·33	0·19	6·84	10·37	2·97	0·19	0·23	2·05	100·27	5·32	7·09	345	127	102	192	97	245	183
429250	Midway 1	1730	48·71	2·32	15·57	12·66	0·20	6·23	11·51	2·40	0·17	0·23	1·60	100·16	4·66	7·13	345	125	92	175	92	266	175
429251	Midway 1	1755	48·73	2·86	13·64	13·97	0·19	6·71	10·68	2·36	0·58	0·28	0·96	100·25	4·29	8·74	411	206	117	221	111	259	219
429252	Midway 1	1800	48·30	2·77	13·73	13·93	0·19	7·19	10·51	2·46	0·65	0·26	2·49	100·52	3·50	9·27	398	266	141	235	104	332	210
458813	Midway 2	1870	48·08	2·73	13·75	13·95	0·20	7·48	10·42	2·73	0·40	0·26	2·14	100·11	2·58	10·12	375	254	167	227	—	368	326
429260	Polar Bear	1775	48·97	2·76	13·55	13·95	0·19	6·66	11·02	2·42	0·22	0·27	1·07	99·93	4·91	8·10	388	260	111	207	109	249	204
429261	Polar Bear	1785	48·62	2·65	13·73	13·72	0·19	7·19	11·10	2·33	0·20	0·27	1·22	100·06	5·91	6·98	385	282	124	197	108	243	202
429262	Polar Bear	1795	49·05	2·76	13·97	13·87	0·19	6·40	10·81	2·49	0·20	0·27	1·11	99·84	6·46	6·60	373	132	102	168	109	253	202
429263	Polar Bear	1815	49·09	2·97	13·15	14·87	0·21	6·02	10·34	2·57	0·48	0·30	0·91	100·09	3·82	9·98	419	88	81	284	124	250	230
'Group 2'																							
429233	Midway 1	1835	48·20	3·27	13·64	14·22	0·20	6·62	10·58	2·50	0·44	0·33	1·28	99·85	4·43	8·75	406	203	113	177	111	296	243
429234	Midway 1	1820	47·98	3·37	13·71	14·47	0·18	6·42	10·86	2·41	0·26	0·34	1·62	99·94	5·55	7·93	437	139	99	251	122	329	251
429253	Midway 1	1820	47·82	3·58	13·26	14·82	0·18	6·53	10·90	2·31	0·26	0·34	1·68	100·07	6·86	7·06	442	127	104	219	121	340	264
429256	Midway 1	1820	48·13	3·47	13·41	14·69	0·19	6·37	10·70	2·44	0·27	0·34	1·38	99·81	5·62	8·08	432	128	97	260	113	319	257
429257	Midway 1	1820	47·91	3·50	13·68	14·56	0·18	6·35	10·87	2·37	0·21	0·36	1·53	100·07	4·55	8·95	438	138	102	256	120	331	265
458819	Midway 2	1922	47·39	3·68	13·27	15·24	0·20	6·70	10·64	2·35	0·20	0·34	1·94	99·79	5·97	8·17	424	117	119	248	—	407	394
458820	Midway 2	1928	47·75	3·30	14·01	14·26	0·20	6·56	10·82	2·53	0·24	0·33	1·26	99·96	5·14	8·15	403	213	178	237	—	409	373
429259	Polar Bear	1775	47·47	3·32	13·80	14·58	0·20	6·81	10·66	2·41	0·43	0·33	1·32	99·95	6·73	6·99	410	207	120	248	118	316	250
Late-stage tholeiitic lavas ('Lindsay Nunatak')																							
429288A	Lindsay	2068	47·01	1·43	9·41	12·86	0·18	18·61	8·72	1·38	0·26	0·16	1·78	99·81	3·17	8·70	240	1678	850	139	73	196	111
429288B	Lindsay	2068	46·77	1·33	8·42	13·15	0·18	20·45	7·80	1·45	0·31	0·13	0·88	99·94	3·08	9·13	219	1682	1022	139	82	198	106
429291	Lindsay	1925	48·44	2·71	9·96	14·10	0·19	11·20	10·05	2·31	0·75	0·32	2·12	99·88	3·23	9·76	303	778	291	134	106	403	207

All analyses by X-ray fluorescence spectrometry on glass discs (except Na_2O and Cu by atomic absorption spectrometry, and FeO by titration) at the Rock Geochemical Laboratory of the Geological Survey of Denmark and Greenland, Copenhagen. Details of analytical procedures and data quality have been given by Kystol & Larsen (1999). Major element data are presented on a volatile-free basis normalized to 100% with total Fe as Fe_2O_3(t), and the totals given are the measured values. 'vol' denotes 'volatiles' and is calculated as the loss on ignition corrected for the calculated gain of weight owing to Fe oxidation during ignition (Kystol & Larsen, 1999). Samples 429288A and 429288B are taken from different parts of the same lava flow. —, element not analysed.

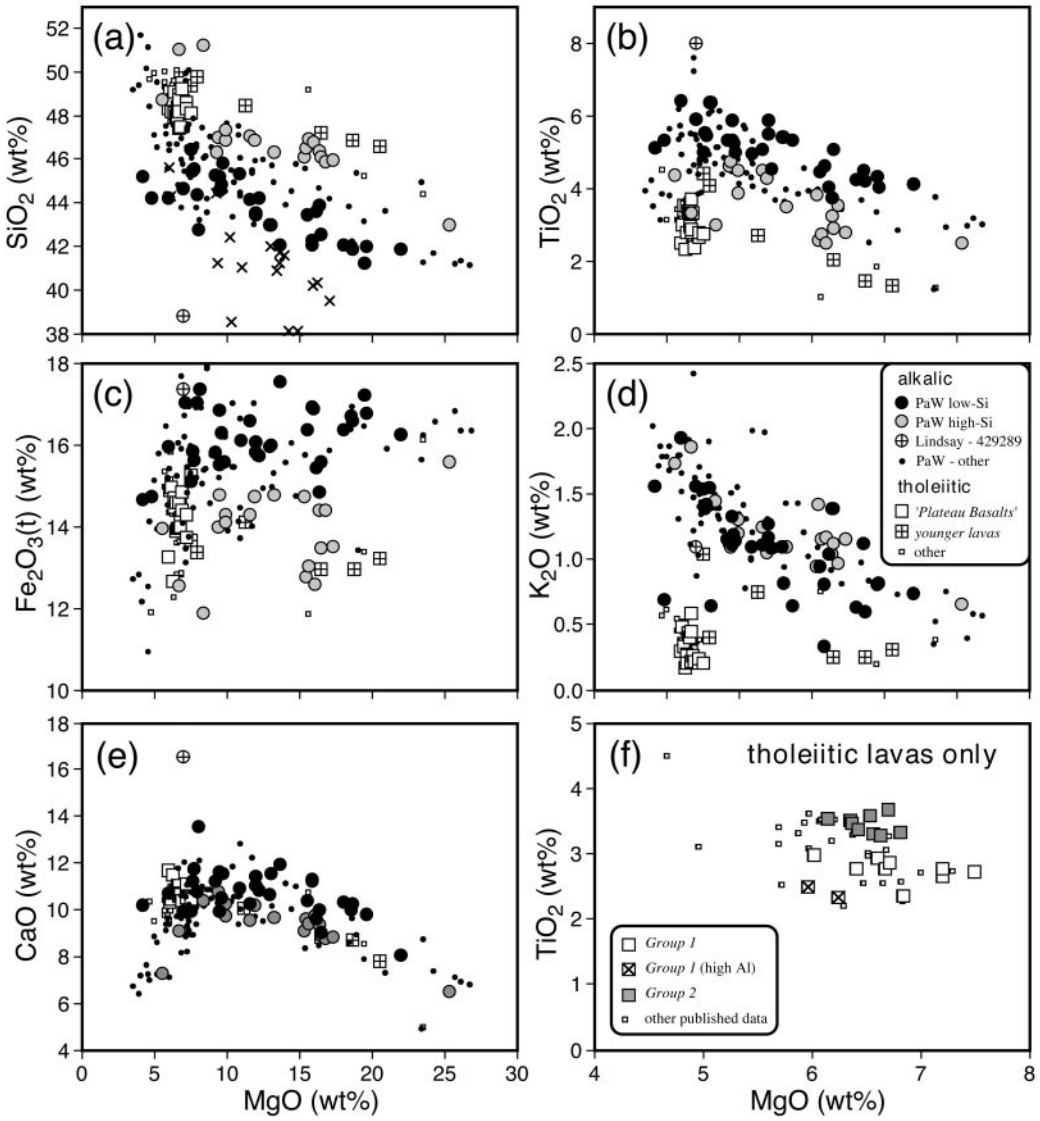

Fig. 4. Major element variation diagrams: MgO vs (a) SiO_2, (b) TiO_2, (c) $Fe_2O_3(t)$, (d) K_2O, (e) CaO (data sources as for Fig. 3). × in (a) represents highly alkaline ultrabasic lavas from the Nunatak Region, NE Greenland (Bernstein *et al.*, 2000). (f) shows an enlarged portion of the MgO vs TiO_2 diagram to highlight the compositional variations just within the lower tholeiitic lavas of the Northern Prinsen af Wales Bjerge.

primitive-mantle-normalized abundances reaching a maximum at Nb and Ta. The Si-enriched group tend to have lower extents of heavy REE (HREE) fractionation, i.e. lower Dy/Yb_N, than the main group (Fig. 6: Dy/Yb_N 1·9–2·3 vs 2·3–2·7). The Si-enriched example plotted in Fig. 5a shows a broadly similar trace element pattern to the main group, but with enrichments in Rb, Ba, K, and especially Pb and Sr.

The 'Lindsay Nunatak' nephelinite has very different trace element characteristics from the other lavas, with much higher incompatible trace element contents, a strongly LREE-enriched pattern (La/Yb_N 49), and marked relative depletions in K, Pb, Sr and P, and low Cs, Rb and Ba (Fig. 5a). These features are also seen in nephelinites from the Gardiner Intrusion (T. F. D. Nielsen & C. K. Brooks, unpublished data, 1997) that is of broadly similar age (56–54 Ma: Waight *et al.*, 2002*b*).

Radiogenic isotopes

Sr, Nd, Pb, Hf and Os isotope data on selected samples are presented in Tables 4 and 5. Additional Sr–Nd–Pb isotope data on lavas from the Prinsen af Wales Bjerge,

Table 3: Trace element data for selected lavas from the Prinsen af Wales Bjerge, East Greenland

Sample	Lab.	Sc	V	Cr	Co	Ni	Cu	Zn	Rb	Sr	Y	Zr	Nb	Cs	Ba	La	Ce	Pr	Nd	Sm	Eu	Gd	Tb	Dy	Ho	Er	Tm	Yb	Lu	Hf	Ta	Pb	Th	U
Alkalic lavas (Prinsen af Wales Bjerge Formation)																																	
Low-Si type																																	
429239	OSU	28	327	329	63	280	191	159	26·2	770	28·0	409	78·4	0·21	341	57·6	133	17·0	69·9	13·3	3·80	10·3	1·47	7·76	1·10	2·84	0·32	1·95	0·26	9·59	5·08	5·84	4·82	1·32
429241	OSU	27	326	789	69	380	187	142	26·5	1026	28·9	429	79·7	0·11	379	58·1	133	16·3	67·8	13·3	3·74	11·0	1·38	6·53	1·08	2·52	0·31	1·83	0·25	10·3	5·18	4·45	4·90	1·50
429241	DUR	28	378	1117	78	473	—	—	30·1	1114	29·5	449	82·3	0·09	393	59·4	135	17·5	66·7	14·1	3·90	10·6	1·35	6·60	1·09	2·46	0·31	1·81	0·25	10·5	5·43	4·31	4·99	1·47
429244	OSU	23	308	1100	85	783	184	145	30·3	1272	22·6	334	67·5	0·39	268	48·7	110	14·1	57·1	11·0	3·11	8·35	1·21	5·96	0·89	2·27	0·24	1·41	0·19	7·95	4·46	3·54	4·51	0·99
429244	DUR	26	331	1456	101	950	—	—	32·7	1457	22·8	334	71·6	0·19	276	51·0	113	14·5	53·8	11·4	3·17	8·52	1·08	5·23	0·86	1·91	0·24	1·37	0·19	8·00	4·85	3·25	4·80	1·08
429244	DUR	24	307	1076	94	893	190	138	30·2	1337	22·2	323	68·6	0·19	285	50·0	108	15·0	60·4	11·0	3·06	8·20	1·10	5·12	0·84	1·85	0·25	1·35	0·19	7·72	4·45	3·15	4·54	1·04
429245	OSU	28	310	763	81	582	220	140	16·9	1535	23·3	293	72·2	0·12	222	46·8	107	12·9	53·4	10·3	2·96	8·65	1·12	5·41	0·85	2·08	0·25	1·50	0·20	6·89	4·68	2·94	4·07	0·97
429294	OSU	26	342	518	77	448	230	150	18·1	1067	25·5	347	73·8	0·11	332	52·2	121	15·0	61·9	12·5	3·59	10·5	1·31	6·30	0·99	2·28	0·26	1·62	0·21	8·19	4·76	3·55	4·29	1·45
429295	OSU	28	384	349	61	135	247	175	25·5	736	34·8	520	78·2	0·16	341	57·1	139	18·6	79·6	16·1	4·54	11·7	1·77	8·81	1·32	3·36	0·37	2·20	0·32	12·1	5·07	4·56	4·78	0·97
429296	OSU	32	360	493	68	241	235	171	20·5	671	30·6	428	70·4	0·13	276	51·9	124	16·4	68·6	13·8	3·94	10·0	1·58	7·82	1·17	2·94	0·35	2·02	0·26	10·3	4·67	3·73	4·24	0·90
429297	OSU	20	344	517	60	221	216	148	21·8	745	27·6	382	76·4	0·21	422	54·1	123	15·1	63·2	12·5	3·59	10·4	1·33	6·52	1·03	2·57	0·31	1·87	0·26	9·10	5·05	4·46	4·14	1·31
429265	DUR	28	316	1504	101	947	166	134	21·6	762	20·5	272	54·5	0·10	209	37·9	86·7	12·4	51·2	9·73	2·72	7·30	0·99	4·71	0·79	1·73	0·24	1·26	0·18	6·78	3·57	2·64	3·30	0·70
429272	OSU	28	316	214	63	353	173	131	15·9	584	26·3	288	45·1	0·14	235	34·8	82·7	10·9	46·0	9·51	2·79	7·47	1·17	6·01	0·99	2·54	0·31	1·92	0·27	6·96	2·99	3·63	4·41	0·73
429299B	OSU	22	367	55	47	76	271	155	34·2	1349	35·8	588	124	0·19	665	88·4	198	24·8	101	19·3	5·48	15·0	1·83	8·61	1·33	3·08	0·36	2·24	0·29	13·4	7·69	7·08	7·79	2·75
436223	OSU	24	336	1076	76	542	211	143	22·9	876	23·0	339	64·0	0·14	288	47·7	111	14·2	57·7	11·2	3·11	8·22	1·25	6·09	0·87	2·31	0·26	1·55	0·21	8·28	4·33	3·76	4·20	0·82
436231	OSU	16	306	9	42	27	192	158	29·0	1311	33·7	424	91·5	0·17	459	69·7	162	20·8	83·6	15·9	4·73	11·7	1·75	8·63	1·28	3·30	0·38	2·26	0·30	10·5	6·02	4·84	6·21	1·18
High-Si type																																	
429235	OSU	22	195	1138	104	1150	130	114	17·1	309	12·9	158	30·0	0·20	155	21·7	49·1	6·47	26·9	5·58	1·62	4·62	0·62	2·93	0·50	1·22	0·15	0·96	0·13	3·89	1·96	2·66	1·50	0·49
429236	OSU	27	267	391	48	124	161	107	28·4	840	18·2	236	42·3	0·17	397	37·2	81·5	10·1	39·7	7·58	2·24	6·67	0·93	4·60	0·70	1·77	0·21	1·34	0·19	5·62	2·67	6·46	3·20	0·50
429237	OSU	25	285	217	45	90	183	115	31·2	576	19·8	268	49·3	0·22	632	42·4	92·3	11·2	43·8	8·23	2·50	7·19	0·97	4·86	0·76	1·99	0·22	1·44	0·20	6·38	3·08	7·49	3·88	0·64
429243	OSU	26	234	660	67	584	165	104	23·5	1319	16·3	187	35·8	0·16	308	28·4	63·0	7·83	31·2	6·00	1·81	5·26	0·76	3·93	0·60	1·63	0·19	1·15	0·17	4·65	2·25	5·13	2·58	0·49
429298	OSU	20	323	11	42	30	57	155	29·9	1172	31·7	415	64·3	0·21	527	53·7	127	16·2	66·5	13·0	3·74	9·96	1·51	7·53	1·18	3·14	0·37	2·29	0·33	9·75	4·19	5·34	4·15	1·17
429258	OSU	21	249	718	66	580	129	115	21·0	594	18·7	197	54·1	0·11	344	37·9	80·9	9·69	37·9	6·82	1·95	6·17	0·81	4·32	0·70	1·89	0·23	1·51	0·21	4·87	3·44	3·98	3·08	0·53
429264	DUR	26	270	1135	83	720	154	114	20·4	848	18·0	230	53·0	0·11	282	37·3	80·3	10·9	43·7	7·91	2·20	5·96	0·81	3·97	0·68	1·55	0·22	1·21	0·18	5·56	3·39	3·24	3·08	0·59
429267	OSU	27	307	172	65	440	173	126	14·7	617	24·8	261	40·4	0·13	202	31·0	73·8	9·77	41·5	8·69	2·57	6·93	1·09	5·63	0·93	2·39	0·30	1·82	0·26	6·35	2·68	3·66	2·87	0·65
429268	OSU	28	314	213	65	402	179	130	14·9	595	25·6	276	43·1	0·12	208	32·8	78·1	10·4	43·9	9·15	2·69	7·20	1·13	5·84	0·96	2·46	0·30	1·86	0·26	6·68	2·85	3·68	2·93	0·66
429273	OSU	27	314	264	64	366	171	130	15·9	597	25·6	280	44·4	0·13	238	34·5	81·6	10·8	45·1	9·25	2·70	7·28	1·14	5·82	0·96	2·49	0·31	1·90	0·27	6·77	2·95	4·58	4·31	0·70
429290	OSU	30	326	292	54	167	165	126	16·9	572	27·2	266	42·8	0·19	236	33·4	78·8	10·4	43·4	9·02	2·68	7·16	1·14	5·93	1·01	2·63	0·33	2·07	0·29	6·45	2·84	3·19	3·75	0·68
Nephelinite ('Lindsay Nunatak')																																	
429289	OSU	24	404	41	50	66	366	176	19·7	1528	47·0	573	222	0·15	797	193	434	53·6	205	35·4	9·14	26·6	2·98	13·2	1·87	4·23	0·46	2·69	0·33	13·1	17·5	7·06	22·7	4·43

Sample	Lab.	Sc	V	Cr	Co	Ni	Cu	Zn	Rb	Sr	Y	Zr	Nb	Cs	Ba	La	Ce	Pr	Nd	Sm	Eu	Gd	Tb	Dy	Ho	Er	Tm	Yb	Lu	Hf	Ta	Pb	Th	U
Late-stage tholeiitic lavas ('Lindsay Nunatak')																																	
429288A	DUR	28	223	1181	84	926	—	—	2·8	202	16·6	97	8·4	0·08	81·0	9·44	22·7	3·18	13·6	3·67	1·17	3·57	0·54	3·12	0·59	1·53	0·22	1·34	0·20	2·54	0·66	1·57	0·69	0·17
429288B	DUR	25	211	1541	93	1091	—	—	4·8	201	15·8	94	8·1	0·05	97·4	9·24	22·1	3·07	13·4	3·55	1·11	3·46	0·51	2·96	0·56	1·46	0·20	1·27	0·19	2·46	0·61	1·50	0·66	0·18
429291	OSU	26	294	726	61	272	118	114	14·4	394	21·6	201	28·4	0·16	206	25·1	59·6	7·95	33·4	7·01	2·13	7·12	0·93	4·76	0·81	2·11	0·27	1·71	0·24	4·93	1·82	2·81	2·02	0·53
429291	DUR	29	303	881	67	321	—	—	15·1	424	21·8	196	29·3	0·15	208	26·0	60·5	8·08	31·9	7·42	2·18	6·22	0·86	4·47	0·81	1·97	0·26	1·59	0·23	4·95	1·94	2·54	2·11	0·55
Tholeiitic lavas (equivalent to the plateau basalt lavas of the Blosseville Kyst)																																	
'Group 1'																																	
429246	OSU	20	296	135	44	74	216	101	2·4	263	25·6	140	9·2	0·38	74·7	10·7	27·4	3·98	19·0	5·07	1·79	5·20	0·87	5·01	0·95	2·48	0·35	2·17	0·32	3·48	0·65	1·57	0·81	0·28
429247	OSU	34	—	145	46	91	212	113	5·5	253	33·7	187	15·2	0·11	55·2	12·7	32·8	4·82	22·8	6·31	2·02	6·57	1·05	6·14	1·23	3·21	0·44	2·89	0·42	4·78	1·04	1·47	1·00	0·29
429250	OSU	31	—	125	45	77	158	100	2·0	262	27·5	144	11·7	0·01	52·6	10·3	26·5	3·95	18·4	5·00	1·74	5·19	0·84	5·07	1·00	2·62	0·36	2·30	0·33	3·66	0·75	1·24	0·81	0·22
429260	OSU	33	—	270	48	99	189	115	1·8	241	31·8	173	15·0	0·01	87·1	13·1	32·2	4·73	21·9	5·88	1·93	6·20	0·97	5·83	1·13	2·92	0·43	2·73	0·41	4·38	1·01	1·63	1·12	0·30
429261	OSU	33	—	291	47	110	177	110	3·0	233	30·8	170	14·4	0·01	79·3	13·1	32·8	4·64	21·0	5·94	1·90	5·95	0·96	5·53	1·11	2·98	0·41	2·62	0·40	4·38	0·95	1·88	1·21	0·27
429262	OSU	31	—	133	47	94	155	115	2·5	244	31·7	172	14·9	0·04	86·1	13·1	32·6	4·60	21·5	5·79	1·87	6·16	0·99	5·67	1·14	3·00	0·42	2·77	0·41	4·37	0·96	1·90	1·21	0·31
429263	OSU	33	—	94	46	70	248	123	8·1	229	34·8	188	16·2	0·05	106	14·0	34·7	4·96	23·1	6·14	1·98	6·51	1·06	6·20	1·26	3·29	0·45	2·91	0·43	4·75	1·03	1·85	1·26	0·34
'Group 2'																																	
429233	OSU	24	372	198	47	97	156	115	5·8	293	31·1	211	20·0	0·03	97·4	15·5	39·9	5·54	25·8	6·77	2·16	6·54	1·07	5·84	1·14	2·99	0·40	2·67	0·37	4·91	1·32	1·63	1·14	0·38
429234	OSU	27	376	141	47	84	221	116	5·4	324	34·9	221	20·9	0·12	73·1	17·0	43·5	5·94	27·8	7·12	2·28	7·15	1·12	6·26	1·22	3·18	0·44	2·85	0·42	5·32	1·33	1·65	1·37	0·39
429253	OSU	34	—	145	48	84	198	127	4·7	326	35·7	229	21·7	0·09	70·5	16·9	43·3	6·25	29·0	7·43	2·30	7·58	1·18	6·56	1·34	3·34	0·46	2·79	0·41	5·75	1·41	1·85	1·44	0·41
429256	OSU	33	—	151	47	86	227	125	5·2	313	35·5	231	21·9	0·06	80·9	17·3	43·8	6·30	29·0	7·33	2·35	7·45	1·17	6·85	1·30	3·44	0·46	2·85	0·42	5·82	1·41	1·86	1·38	0·40
429257	OSU	32	—	150	48	90	225	126	3·7	316	36·4	234	21·7	0·06	65·3	17·3	43·9	6·36	29·0	7·49	2·40	7·43	1·17	6·72	1·30	3·34	0·46	2·88	0·44	5·74	1·43	1·84	1·48	0·42
429259	OSU	32	—	230	48	106	225	124	4·4	305	34·6	220	20·4	0·01	101	16·4	41·5	6·02	27·1	7·23	2·25	7·21	1·13	6·41	1·23	3·20	0·45	2·83	0·41	5·38	1·34	2·09	1·43	0·33
Internal standard (GGU95358—basalt from Kap Stosch, East Greenland)																																	
95358	OSU	39	324	188	47	81	167	98	4·8	204	30·3	119	9·0	0·11	55·4	8·02	20·7	3·10	15·0	4·47	1·56	5·07	0·86	5·20	1·08	2·82	0·41	2·68	0·39	3·07	0·70	1·03	0·68	0·20
$n = 24$	± SD	2	14	9	2	3	4	3	0·1	4	0·4	2	0·4	0·01	0·8	0·20	0·5	0·04	0·3	0·11	0·03	0·17	0·02	0·11	0·03	0·05	0·01	0·07	0·01	0·07	0·02	0·06	0·03	0·02
95358	DUR	40	338	206	50	90	—	—	4·8	208	30·4	117	9·2	0·10	55·6	8·16	20·8	3·16	15·1	4·64	1·62	5·24	0·90	5·41	1·09	2·87	0·43	2·63	0·41	3·10	0·77	0·93	0·72	0·20
$n = 9$	± SD	1	6	14	1	2	—	—	0·1	5	0·3	1	0·5	0·01	1·1	0·12	0·3	0·06	0·5	0·05	0·03	0·06	0·02	0·06	0·02	0·04	0·02	0·02	0·01	0·02	0·01	0·12	0·04	0·01

All analyses by ICP-MS at the University of Oregon, USA (OSU) or the University of Durham, UK (DUR). Bernstein *et al.* (2001) and Peate *et al.* (2001) have given details of the analytical methods and estimates of accuracy and precision for the Oregon and Durham laboratories, respectively. GGU95358 is an internal standard rock (basalt from Kap Stosch, East Greenland) that was run numerous times interspersed with unknown samples at both laboratories to check reproducibility and any inter-laboratory biases.

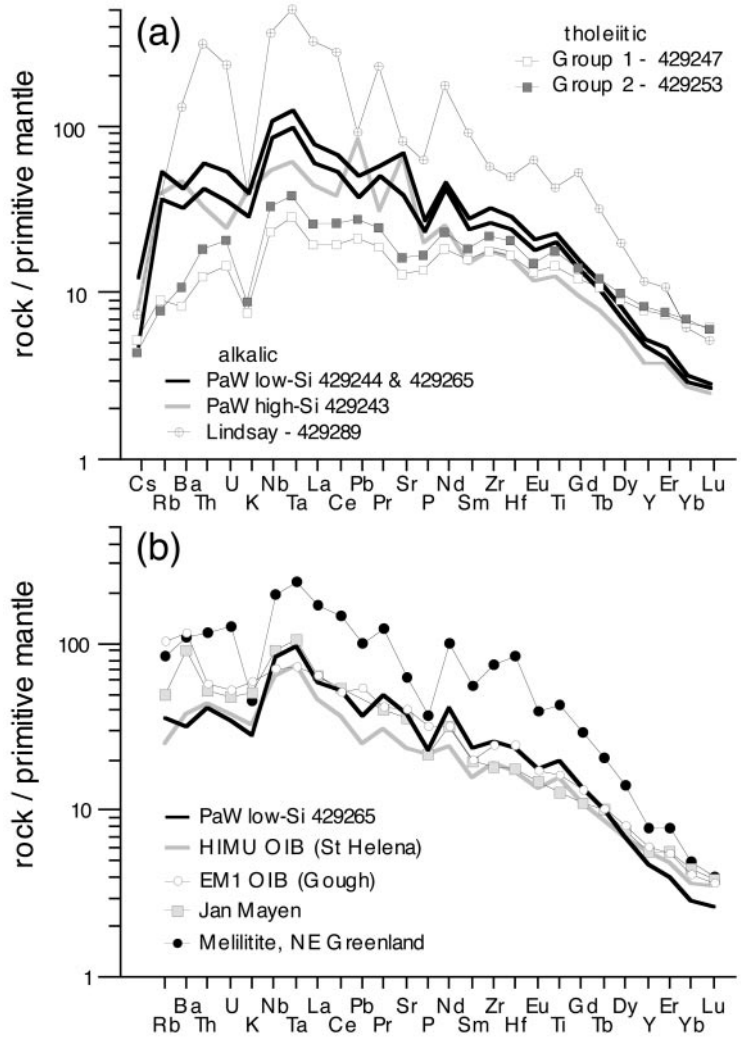

Fig. 5. Primitive-mantle-normalized trace element diagrams [normalizing values from Sun & McDonough (1989)]: (a) for representative samples of each principal compositional type in the Prinsen af Wales Bjerge; (b) comparison of Prinsen af Wales Bjerge alkalic lava with other 'enriched' magmas: melilitite, Nunatak Region, NE Greenland (Bernstein *et al.*, 2001); Jan Mayen ankaramite (Trønnes *et al.*, 1999); St. Helena HIMU OIB (Chaffey *et al.*, 1989; Thirlwall, 1997); Gough EMI OIB (Sun & McDonough, 1989).

Trekantnunatakker, and 'Lindsay Nunatak' have been given by Brown *et al.* (1996, 2000) and Ellam & Stuart (2000). The Sr–Nd–Pb isotope data are illustrated in Fig. 7, which includes fields for data from the plateau basalts, Lower Basalts, offshore SE Greenland basalts and Iceland for comparison. The data from Brown *et al.* (1996, 2000) show slightly elevated $^{87}Sr/^{86}Sr_i$ compared with the data in this study (Fig. 7a), which is probably due to their samples not being leached before analysis.

The tholeiitic lavas have $^{87}Sr/^{86}Sr_i$ of 0·7032–0·7048, εNd_i of +4·7 to +7·6, and $^{206}Pb/^{204}Pb$ of 17·1–18·3, consistent with existing data on the coastal plateau basalts (Brown *et al.*, 1996; Peate & Stecher, 2002; Andreasen *et al.*, in preparation;). The young tholeiitic flow from 'Lindsay Nunatak' has high $^{87}Sr/^{86}Sr_i$ of 0·7063, low εNd_i of −2·0, and very unradiogenic $^{206}Pb/^{204}Pb$ of 15. The alkalic lavas, in general, have higher $^{87}Sr/^{86}Sr_i$ (0·7037–0·7061) and lower εNd_i (−1·6 to +6·2) than the tholeiitic lavas. They show a wide range in Pb isotope composition, with $^{206}Pb/^{204}Pb$ varying from 14·7 to 18·5, but appear to be offset to lower $^{207}Pb/^{204}Pb$ relative to the tholeiitic lavas and coastal plateau basalts. This is not an analytical effect, as alkalic and tholeiitic samples were run interspersed in the same analytical session. The extreme

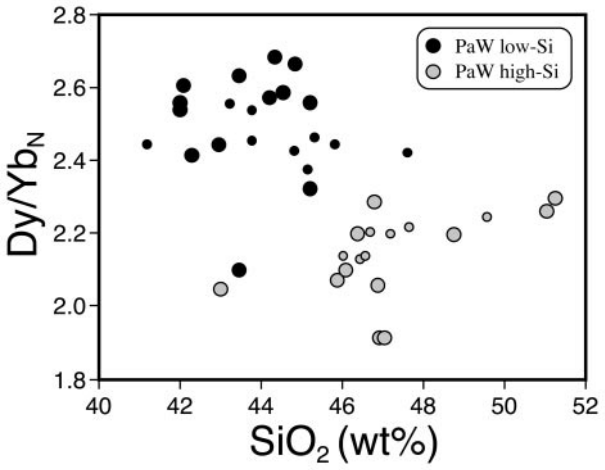

Fig. 6. SiO_2 vs Dy/Yb_N for the Prinsen af Wales Bjerge Formation alkalic lavas. Small symbols are analyses from 1982 Nunatak (Hansen *et al.*, 2002).

isotopic variations, particularly in Pb isotopic compositions, seen in the alkalic lavas and some of the tholeiitic lavas are probably due to crustal assimilation with an unradiogenic Pb component (see discussion below). In terms of Hf and Nd isotopes, the Prinsen af Wales Bjerge lavas all lie below the 'mantle array' (Fig. 8a: Vervoort *et al.*, 1999), with low εNd_i and εHf_i relative to published data on Icelandic lavas and crustally uncontaminated samples related to the North Atlantic break-up (Kempton *et al.*, 2000). The 'Lindsay Nunatak' nephelinite has a similar Sr, Nd and Hf isotope composition to the least contaminated Prinsen af Wales Bjerge alkalic rocks, but it has a very different Pb isotope composition, with an extremely radiogenic $^{206}Pb/^{204}Pb$ of 23 (not shown in Fig. 7).

Six Prinsen af Wales Bjerge alkalic lavas were analysed for Os concentrations and isotope compositions. All samples have relatively high Os abundances from 0·17 to 1·17 ppb, and they have a range in $^{187}Os/^{188}Os_i$ from 0·120 to 0·132. It should be noted that the sample with the lowest $^{187}Os/^{188}Os_i$ (429244: $^{187}Os/^{188}Os_i$ 0·120), also has the lowest Os content and highest Re/Os of all the samples, and its low initial Os isotope ratio might just be the result of an erroneously large age-correction owing to late-stage Re addition. The observed range in initial Os isotope compositions overlaps with the known range of Icelandic lavas ($^{187}Os/^{188}Os$ 0·127–0·137: Skovgaard *et al.*, 2001; Smit *et al.*, 2001), although extending to subchondritic values lower than any known Iceland sample (Fig. 8b). $^{187}Os/^{188}Os_i$ values as low as 0·122 have been measured in ~61 Ma lavas from Baffin Island (A. J. R. Kent, unpublished data, 2001), albeit with significantly higher εNd_i than the Prinsen af Wales Bjerge samples (Fig. 8b).

Helium isotopes

In general, Icelandic basalts are characterized by $^3He/^4He$ values higher than those found in mid-ocean ridge basalt (MORB) ($R/R_A = 8 \pm 1$: Farley & Neroda, 1998), indicating a source component derived from a region with higher time-integrated $^3He/(U + Th)$ than the convecting upper mantle, and usually inferred to be the lower mantle (e.g. Condomines *et al.*, 1983; Kurz *et al.*, 1985; Poreda *et al.*, 1986; Hilton *et al.*, 1999; Breddam *et al.*, 2000). Thus, He isotopes can potentially be used as a tracer of the contribution of Icelandic plume mantle to the Palaeogene North Atlantic magmatism. $^3He/^4He$ values greater than those of MORB have been found in early phase lavas in West Greenland ($R/R_A = 31$; Graham *et al.*, 1998), NE Greenland ($R/R_A = 21$; Marty *et al.*, 1998) and Scotland ($R/R_A = 22$; Stuart *et al.*, 2000). No studies have yet been carried out on East Greenland lavas of either the initial or main magmatic episodes. Single $^3He/^4He$ values of 10·8 (Lilloise intrusion: Bernstein *et al.*, 1998*b*) and 10·5 (Prinsen af Wales Bjerge: Ellam & Stuart, 2000) have been measured in olivines from the post break-up magmatic episode, but these values are barely resolvable within error from the canonical MORB range (Farley & Neroda, 1998).

We report new helium isotope data on separated olivines from four Prinsen af Wales Bjerge alkalic lavas in Table 5. Analyses were carried out by crushing *in vacuo* so as to liberate helium trapped in inclusions within the olivine crystals. This technique gives the best estimates for the magmatic helium isotope signature, although the results probably represent minimum values (e.g. Hilton *et al.*, 1999). Three samples show $^3He/^4He$ isotope ratios clearly elevated with respect to MORB (R/R_A 12·4, 16·0, 18·5) and the fourth sample has a low $^3He/^4He$ value (R/R_A 4·9). The new He and Pb isotope data on the Prinsen af Wales Bjerge lavas combined with those of Ellam & Stuart (2000) fall on a broad hyperbolic trend with the low $^3He/^4He$ samples (R/R_A 1·8–9·7) having unradiogenic $^{206}Pb/^{204}Pb$ (14·7–17·6) consistent with assimilation of radiogenic ^4He-bearing, low $^{206}Pb/^{204}Pb$ crustal material (Fig. 9). These data represent the first clear evidence for a high $^3He/^4He$ component present in Palaeogene lavas from the Kangerlussuaq region, which lies on the hotspot track of the Iceland plume axis (Lawver & Müller, 1994; Torsvik *et al.*, 2001).

Olivine compositions

We carried out a reconnaissance survey of olivine compositions in the Prinsen af Wales Bjerge Formation alkalic lavas to look for possible xenocrystic lithospheric mantle olivines. The four analysed samples show a similar range of core olivine compositions (Fig. 10: $Fo_{85·0–89·4}$; $n = 66$: sample 429264 has two olivines with Fo_{78}). Crystal zoning appears to be limited, and in all cases is normal. However,

Table 4: Sr–Nd–Pb isotope data for selected lavas from the Prinsen af Wales Bjerge, East Greenland

Sample	$^{87}Sr/^{86}Sr$ measured	$^{143}Nd/^{144}Nd$ measured	$^{143}Nd/^{144}Nd$ initial	ε_{Nd} init.	$^{206}Pb/^{204}Pb$ measured	$^{207}Pb/^{204}Pb$ measured	$^{208}Pb/^{204}Pb$ measured	$^{206}Pb/^{204}Pb$ initial	$^{207}Pb/^{204}Pb$ initial	$^{208}Pb/^{204}Pb$ initial
Alkalic lavas (Prinsen af Wales Bjerge Formation)—low-Si type										
429244	0·70405	0·512825	0·51278	4·1	18·442	15·265	38·737	18·28	15·26	38·51
429265	0·70369	0·512817	0·51278	4·0	18·527	15·305	38·513	18·39	15·30	38·30
429272	0·70386	0·512843	0·51280	4·4	18·479	15·330	38·505	18·37	15·32	38·37
429241	0·70406	0·512722	0·51268	2·1	18·358	15·294	38·153	18·17	15·29	37·95
429296	0·70412	0·512752	0·51271	2·7	17·686	15·169	37·486	17·57	15·16	37·32
Alkalic lavas (Prinsen af Wales Bjerge Formation)—high-Si type										
429235	0·70500	0·512743	0·51270	2·5	17·022	15·002	37·579	16·93	15·00	37·48
429264	0·70500	0·512702	0·51266	1·8	16·599	14·959	36·934	16·51	14·95	36·78
429258	0·70430	0·512557	0·51252	−1·0	16·970	15·001	36·923	16·91	15·00	36·81
429243	0·70608	0·512530	0·51249	−1·6	16·771	14·928	37·451	16·73	14·93	37·38
Nephelinite ('Lindsay Nunatak')										
429289	0·70373	0·512845	0·51281	4·6	23·228	15·623	47·098	22·78	15·60	46·32
Late-stage tholeiitic lavas ('Lindsay Nunatak')										
429288A	0·70627	0·512526	0·51247	−2·0	14·971	14·662	35·171	14·92	14·66	35·10
429291	0·70477	0·512645	0·51260	0·5	16·207	14·906	36·258	16·11	14·90	36·14
Tholeiitic lavas (equivalent to plateau basalt lavas of the Blosseville Kyst)—'group 1'										
429247	0·70318	0·513018	0·51296	7·6	18·135	15·386	37·961	18·03	15·38	37·85
429261	0·70480	0·512871	0·51281	4·7	17·071	15·195	37·728	17·00	15·19	37·63
Tholeiitic lavas (equivalent to plateau basalt lavas of the Blosseville Kyst)—'group 2'										
429253	0·70334	0·512985	0·51293	7·0	18·263	15·426	38·317	18·15	15·42	38·19
429259	0·70332	0·513004	0·51295	7·3	18·230	15·392	38·140	18·15	15·39	38·03

Sr–Nd–Pb isotope analyses were carried out on an Axiom multi-collector (MC)-ICP-MS at the Danish Lithosphere Centre. Sr isotopes were determined on powders, leached in warm 6M HCl for ~2 h. Sr was separated using cation ion-exchange followed by clean-up with Eichrom Sr-spec resin to remove any remaining Rb and also HREE that can form doubly charged species and interfere (1) on mass 85, resulting in an over-correction for the ^{87}Rb interference on ^{87}Sr, and (2) at half mass units, limiting the effectiveness of standard background measurement procedures. Thus, Sr isotope ratios were measured using an on-peak zero method rather than at half mass unit offsets to avoid such interferences and to minimize the effect of Kr interference on ^{86}Sr. $^{87}Sr/^{86}Sr$ data were corrected for mass fractionation using $^{86}Sr/^{88}Sr = 0{\cdot}1194$. Further details of the Sr analytical technique have been given by Waight *et al.* (2002*a*). The samples were run in one analytical session during which SRM987 gave $^{87}Sr/^{86}Sr = 0{\cdot}710251 \pm 15$ (2 SD, $n = 5$), and E&A gave $^{87}Sr/^{86}Sr = 0{\cdot}708009 \pm 15$ (2 SD, $n = 5$). The $^{87}Sr/^{86}Sr$ data are presented relative to $^{87}Sr/^{86}Sr = 0{\cdot}71025$ for SRM987. Nd isotopes were measured on unleached powders, using the REE column cuts from the Sr cation ion-exchange column. Unseparated Sm–Nd fractions were first cleaned of residual Ba using a micro-cation column, and then analysed following the general technique of Luais *et al.* (1997). Isotope ratios were corrected for mass fractionation using $^{146}Nd/^{145}Nd = 2{\cdot}071943$ as both these masses are free of Sm isobaric interferences. The samples were all run in a single analytical session, during which the Ames Nd metal std gave $^{143}Nd/^{144}Nd = 0{\cdot}512120 \pm 10$ (2 SD, $n = 7$). The $^{143}Nd/^{144}Nd$ data are presented relative to an Ames Nd metal std value of $^{143}Nd/^{144}Nd = 0{\cdot}51213$ (equivalent to a La Jolla Nd standard value of $^{143}Nd/^{144}Nd = 0{\cdot}51185$: E. J. Krogstad, personal communication, 2001). Pb isotope analyses were performed on hand-picked rock chips, leached in 6M HCl on a hot plate for ~2 h. Mass fractionation was corrected during the run by using the Tl-doping method, with a Tl/Pb value of ~0·2. A $^{203}Tl/^{205}Tl$ value of 0·41855 yields Pb isotope ratios for SRM981 of $^{206}Pb/^{204}Pb$ 16·941 ± 0·003, $^{207}Pb/^{204}Pb$ 15·498 ± 0·004, $^{208}Pb/^{204}Pb$ 36·722 ± 0·012, with collector efficiencies all set to one (all errors are 2 SD). These values for SRM981 are in good agreement with those determined by Thirlwall (2000) using the ^{207}Pb–^{204}Pb double spike method ($^{206}Pb/^{204}Pb$ 16·941 ± 0·002, $^{207}Pb/^{204}Pb$ 15·496 ± 0·003, $^{208}Pb/^{204}Pb$ 36·723 ± 0·008). Initial ratios calculated back to an age of 53 Ma. Parent/daughter elemental ratios were not measured on the acid-leached residues for the Sr and Pb analyses, but following the arguments given by Thirlwall *et al.* (1994), we use U/Pb and Th/Pb values measured in the unleached powders by ICP-MS (Table 3) to age correct the Pb isotope data and make no age correction to the Sr isotope data. Measured Rb/Sr values are low (0·01–0·06), which would result in a maximum correction to the measured $^{87}Sr/^{86}Sr$ value of 0·00013, and Rb/Sr in the leached residues are likely to be even lower (see also Fitton *et al.*, 1998; Saunders *et al.*, 1999).

Table 5: Hf–Os–He isotope data for selected lavas from the Prinsen af Wales Bjerge, East Greenland

Sample	$^{176}Hf/^{177}Hf$ measured	ε_{Hf} meas.	ε_{Hf} init.	Re (ppt)	Os (ppt)	$^{187}Os/^{188}Os$ measured	$^{187}Os/^{188}Os$ initial	γ_{Os} init.	$^{3}He/^{4}He$ R/R_A $\pm$ 1σ	[He] $\times 10^{-9}$ cm^3 STP/g
Alkalic lavas (Prinsen af Wales Bjerge Formation)—low-Si type										
429244	0·282935 ± 5	5·76	6·84	239	169	0·1261	0·1201	−6·6	12·2 ± 0·2	8·73 ± 0·15
429265	0·282923 ± 5	5·34	6·41	191	503	0·1261	0·1245	−3·2	18·1 ± 0·2	7·25 ± 0·12
429272	0·282941 ± 5	5·98	6·98	—	—	—	—	—	15·6 ± 0·2	5·87 ± 0·10
429241	0·282873 ± 5	3·57	4·65	51	1168	0·1258	0·1257	−2·3	—	—
429296	0·282842 ± 5	2·48	3·55	—	—	—	—	—	—	—
Alkalic lavas (Prinsen af Wales Bjerge Formation)—high-Si type										
429235	0·282842 ± 7	2·48	3·51	n.a.	710	0·1237	0·1237	−3·8	—	—
429264	0·282771 ± 5	−0·04	0·96	37	943	0·1302	0·1300	1·1	4·8 ± 0·1	13·2 ± 0·2
429258	0·282708 ± 7	−2·26	−1·28	—	—	—	—	—	—	—
429243	0·282670 ± 4	−3·61	−2·59	14	331	0·1315	0·1314	2·1	—	—
Nephelinite ('Lindsay Nunatak')										
429289	0·282955 ± 7	6·47	7·54	—	—	—	—	—	—	—
Late-stage tholeiitic lavas ('Lindsay Nunatak')										
429288A	0·282683 ± 7	−3·15	−2·34	—	—	—	—	—	—	—
429291	0·282755 ± 6	−0·06	0·35	—	—	—	—	—	—	—

Initial Hf and Os isotope ratios calculated at 53 Ma. *Hafnium isotopes*: Hf isotope compositions were determined by MC-ICP-MS (VG Plasma 54) at the École Normale Supérieure de Lyon using the method described by Blichert-Toft *et al.* (1997). Because of the Mg-rich nature of these samples, Hf was separated following the protocol outlined by Blichert-Toft (2001), which is a slightly modified version of the procedure originally described by Blichert-Toft *et al.* (1997). The JMC475 Hf standard gave $^{176}Hf/^{177}Hf = 0{\cdot}282160 \pm 10$ (2 SD) and was analysed alternately with the samples: in-run errors are better than ± 10 for all samples. Data are normalized for mass fractionation using $^{179}Hf/^{177}Hf = 0{\cdot}7325$. ε_{Hf} values are calculated using $(^{176}Hf/^{177}Hf)_{CHUR(0)} = 0{\cdot}282772$, $(^{176}Lu/^{177}Hf)_{CHUR(0)} = 0{\cdot}0332$, and $\lambda_{Lu} = 1{\cdot}93 \times 10^{-11}$ a^{-1}. *Osmium isotopes*: Os concentrations and isotope compositions were analysed at the Danish Centre for Isotope Geology, Geological Institute, University of Copenhagen. Re concentrations were determined by MC-ICP-MS (NuPlasma) at the University of Bern, using an isotope dilution method (Schoenberg *et al.*, 2000). Re and Os data were determined on the same sample digestion. Samples were spiked with Re and Os tracer solutions and digested in inverse aqua regia in Carius tubes for >72 h at 200°C, followed by microdistillation using the technique outlined by Nägler & Frei (1997). Os isotopic compositions were measured by negative thermal ionization mass spectrometry (N-TIMS) using the Faraday collectors [mass spectrometry details have been given by Hanghøj *et al.* (2001)]. Blanks: Re 50 pg, Os <2 pg. Re was not analysed for sample 429235, and so the calculated initial Os isotope ratios are maximum values. γ_{Os} values are calculated using $^{187}Re/^{188}Os_{mantle} = 0{\cdot}428$, $^{187}Os/^{188}Os_{mantle} = 0{\cdot}1290$, and $\lambda_{Re} = 1{\cdot}666 \times 10^{-11}$ a^{-1} (Meisel *et al.*, 1996; Smoliar *et al.*, 1996). *Helium isotopes*: helium was liberated from olivine phenocrysts by on-line crushing [see Scarsi (2000) for description of the apparatus]. Crushing times were limited to ~2 min to avoid potential release of matrix-sited helium components (Hilton *et al.*, 1999). Helium isotope analyses were carried out using a MAP 215 noble gas mass spectrometer at the Scripps Institution of Oceanography. Helium from Murdering Mudpots, Yellowstone Park (16·45 R_A) was used as the normalizing standard.

two samples contain rare olivines with more magnesian compositions: 429235 ($Fo_{91·0}$ and $Fo_{91·6}$) and 429244 ($Fo_{93·2}$). The question is whether these Mg-rich olivines crystallized from melts or represent mantle olivine xenocrysts. Mantle olivines have low CaO and Cr_2O_3 contents relative to magmatic olivines (e.g. Gurenko *et al.*, 1996; Larsen & Pedersen, 2000). Analyses of local lithospheric mantle olivines are available from xenoliths in ~40 Ma dykes from Wiedemann Fjord (Fig. 1: Bernstein *et al.*, 1998*a*). The Prinsen af Wales Bjerge and xenolith data are plotted in Fig. 10 together with a reference suite of magmatic olivines (West Greenland picrites: Larsen & Pedersen, 2000). Only one analysed olivine (the one with the highest Fo content) has suitably low Cr_2O_3 to make it a possible xenocrystic lithospheric mantle olivine, although its CaO content, while low, is still higher than that of most mantle olivines.

DISCUSSION

Stratigraphic relationship of the tholeiitic lavas to the coastal plateau basalts

The ^{40}Ar–^{39}Ar age for the 'Lindsay Nunatak' alkalic lava is younger than the plateau basalts (56–54 Ma: Storey *et*

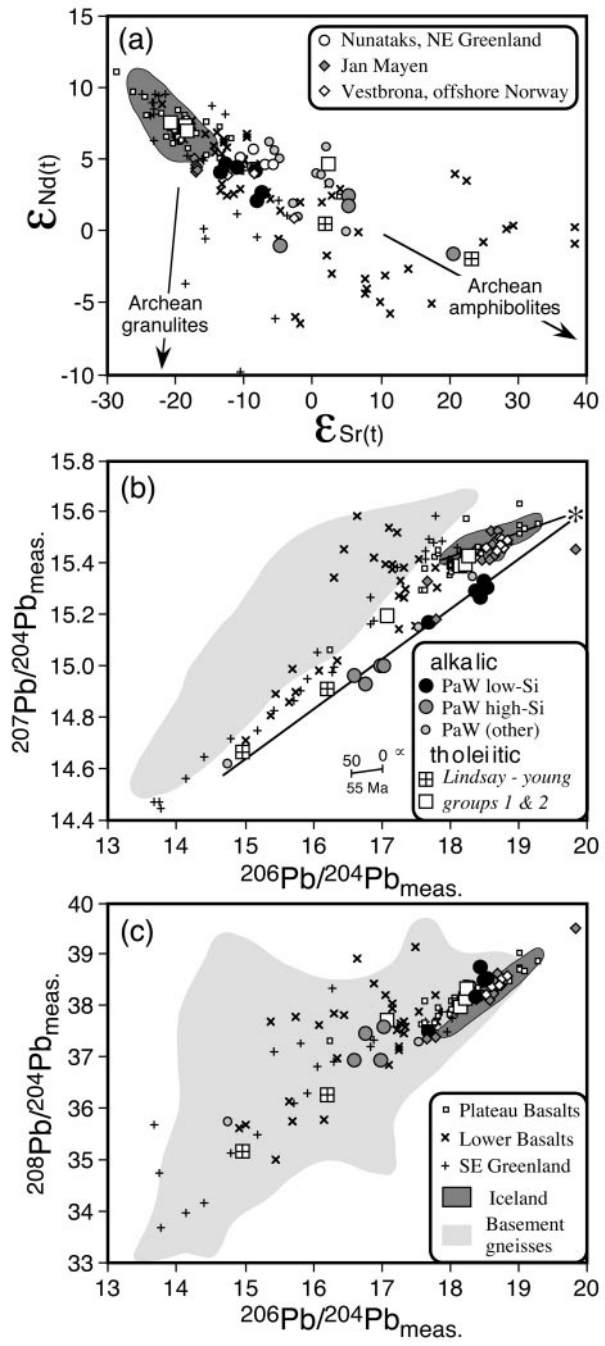

al., 1996; Heister *et al.*, 2001; Hansen *et al.*, 2002). However, alkalic lavas are found interbedded with tholeiitic lavas at Midway Nunatak (Fig. 2) and Tjeldebjerge (Fig. 1: Anwar 1955), although lavas from these sections have yet to be dated. If these tholeiitic lavas can be correlated with the coastal plateau basalt stratigraphy, this would place a maximum age on the initiation of alkalic magmatism. The 55 Ma age for the vent sample already suggests that some alkalic magmatism was contemporaneous with the plateau basalts. Hansen *et al.* (2002) showed from compositional criteria and photogrammetric studies that most of the tholeiitic lavas in the Urbjerget region are equivalent to the lowermost plateau basalts (Milne Land Formation: Larsen *et al.*, 1989; Pedersen *et al.*, 1997). The tholeiitic lavas in the northern Prinsen af Wales Bjerge should lie stratigraphically above those at Urbjerget, given the general northward dip of the plateau basalts in this area, and are thus most likely to represent either the upper part of the Milne Land Formation or the overlying Geikie Plateau Formation.

It might be possible to use distinctive compositional features to correlate the lavas with a particular plateau basalt formation. For example, using samples from a 6 km composite section through the coastal plateau basalts at Sortebræ (Fig. 1), Tegner *et al.* (1998*b*) demonstrated a contrasting behaviour in REE systematics between the lower and upper parts. In the lower part (Milne Land and Geikie Plateau Formations), there is a negative correlation of Dy/Yb_N with La/Sm_N, whereas in the upper part (Rømer Fjord and Skrænterne Formations), these ratios show a positive correlation (Fig. 11a). Furthermore, within the lower part, there are systematic variations with stratigraphic height, with La/Sm_N increasing and Dy/Yb_N decreasing up through the Milne Land and Geikie Plateau Formations.

The main Group 1 tholeiites have higher La/Sm_N and lower Dy/Yb_N than the stratigraphically lower Urbjerget tholeiites that are clearly equivalent to the lower Milne Land Formation (Fig. 11a: Hansen *et al.*, 2002). This stratigraphic compositional transition in the inland area from the Urbjerget tholeiites to the Group 1 tholeiites appears to be equivalent to the temporal variations within

Fig. 7. Radiogenic isotope variations. (a) $\varepsilon Sr_{(t)}$ vs εNd_t; (b) $^{206}Pb/^{204}Pb_{meas.}$ vs $^{207}Pb/^{204}Pb_{meas}$; (c) $^{206}Pb/^{204}Pb_{meas.}$ vs $^{208}Pb/^{204}Pb_{meas.}$. The symbol legends apply to all three figures. Data sources: Prinsen af Wales Bjerge region alkalic and tholeiitic lavas (this study; Brown *et al.*, 1996, 2000; Ellam & Stuart, 2000); plateau basalts (Brown *et al.*, 1996; Peate & Stecher, 2002; Andreasen *et al.*, in preparation) Lower Basalts (Holm, 1988; Fram & Lesher, 1997; Hansen & Nielsen, 1999); offshore SE Greenland (Fitton *et al.*, 1998; Saunders *et al.*, 1999); Iceland (Sun & Jahn, 1975; Hémond *et al.*, 1993; Hards *et al.*, 1995; Hanan & Schilling, 1997; Hardarson *et al.*, 1997; Stecher *et al.*, 1999; Chauvel & Hémond, 2000); NE Greenland Nunatak lavas (Bernstein *et al.*, 2000, 2001); Jan Mayen (Trønnes *et al.*, 1999); Vestbrona nephelinites (56 Ma, offshore Norway—Prestvik *et al.*, 1999); Archaean basement Pb isotopes (Leeman *et al.*, 1976; Taylor *et al.*, 1992; Kalsbeek *et al.*, 1993). Archaean granulite gneiss has $\varepsilon Sr_{60} \sim -24$ and $\varepsilon Nd_{60} \sim -35$ and Archaean amphibolite gneiss has $\varepsilon Sr_{60} \sim 170$ and $\varepsilon Nd_{60} \sim -42$ [end-member compositions from Saunders *et al.* (1999)]. Sample 429289 is not plotted on the Pb isotope diagrams because of its extreme $^{206}Pb/^{204}Pb$ value of ~ 23. The lines in (b) are regression lines through the Prinsen af Wales Bjerge lava data and the literature Iceland basalt data respectively, and the asterisk marks the point of intersection, which is a reasonable estimate for the composition of an uncontaminated Prinsen af Wales Bjerge alkalic magma.

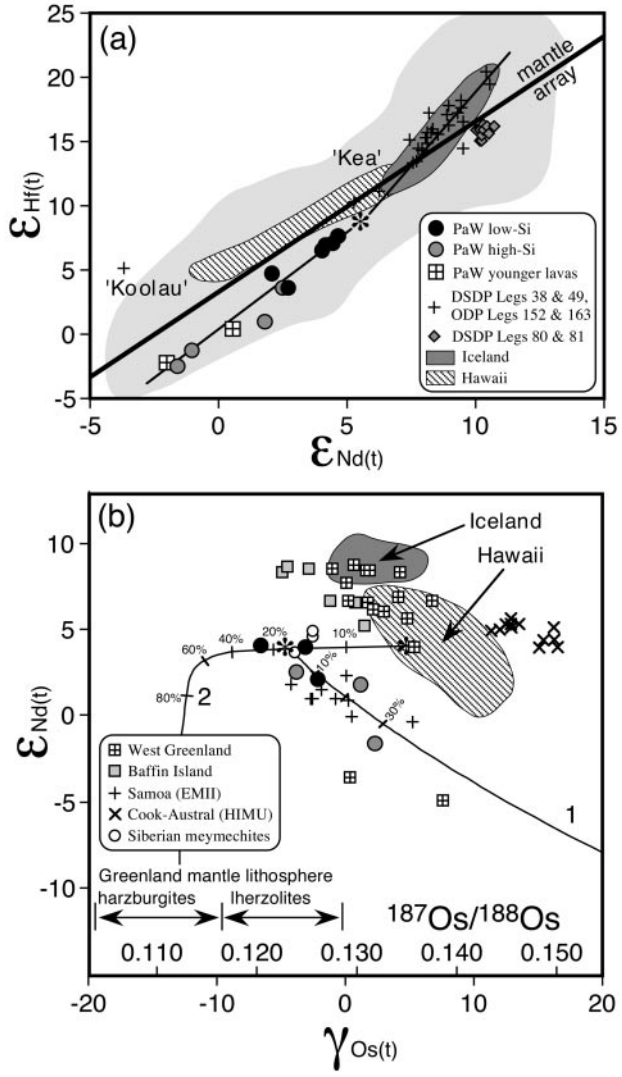

Fig. 8. (a) εNd(t) vs εHf(t). Global MORB–OIB field (light shaded area) and 'mantle array' from Vervoort *et al.* (1999) and J. Blichert-Toft (unpublished data, 2002). The asterisk marks the inferred composition of the uncontaminated Prinsen af Wales Bjerge alkalic lava, and it lies on an extension of the steep Icelandic data trend. 'Kea' and 'Koolau' refer to the high-εNd and low-εNd components of the Hawaii plume, respectively. Data sources: Blichert-Toft *et al.* (1999); Kempton *et al.* (2000); Hanan *et al.* (2000). (b) γOs(t) vs εNd(t). Data sources: Baffin Island (A. J. R. Kent, unpublished data, 2001), West Greenland (Schaefer *et al.*, 2000), Iceland (Skovgaard *et al.*, 2001), East Greenland lithospheric mantle (Wiedemann xenoliths: Hanghøj *et al.*, 2001), Siberian meymechites (Horan *et al.*, 1995), Hawaii (Bennett *et al.*, 1996), Samoa and Cook–Austral (Hauri & Hart, 1993). Curve 1 represents mixing between a primitive Prinsen af Wales Bjerge magma and continental crust, and curve 2 represents mixing between an 'enriched' plume component, as represented by the Palaeogene Baffin Island and West Greenland data, and lithospheric mantle. End-member parameters: Prinsen af Wales Bjerge magma: Os 1 ppb, γOs_i −5, Nd 50 ppm, εNd_i +4; 'enriched plume': same as for Prinsen af Wales magma but with γOs_i +5; continental crust: Os 10 ppt, γOs_i 1448, Nd 10 ppm, εNd_i −42; lithospheric mantle: Os 3·5 ppb, γOs_i −13, Nd 1 ppm, εNd_i −15 (McDonough & Sun, 1995; Saunders *et al.*, 1999; Schaefer *et al.*, 2000).

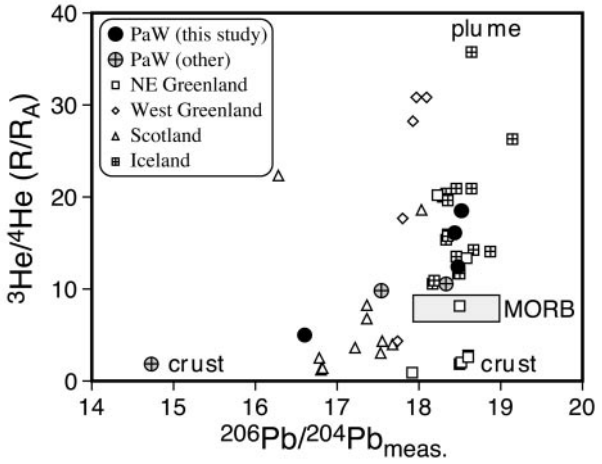

Fig. 9. $^{3}He/^{4}He$ (R/R_A) in olivines vs $^{206}Pb/^{204}Pb$ in host lava. Data sources: Prinsen af Wales Bjerge ~53 Ma (this study; Ellam & Stuart, 2000); West Greenland ~61 Ma (Graham *et al.*, 1998); NE Greenland ~58 Ma (Thirlwall *et al.*, 1994; Marty *et al.*, 1998); Isle of Skye, Scotland, ~61 Ma (Stuart *et al.*, 2000); Iceland ~15–0 Ma (Hilton *et al.*, 1999; Breddam *et al.*, 2000). Average crust in East Greenland and Scotland has $^{206}Pb/^{204}Pb$ ~14·5 and R/R_A ~0·02 (Stuart *et al.*, 2000), whereas crust in NE Greenland has more radiogenic $^{206}Pb/^{204}Pb$ ~18·6 (Thirlwall *et al.*, 1994).

the lower part of the plateau basalts, suggesting that the Group 1 tholeiites are equivalent to the upper Milne Land or Geikie Plateau Formations. The relatively low La/Sm_N of the Group 1 tholeiites rules out any correlation with the Rømer Fjord Formation lavas. There is an overlap in REE compositions with some lavas from the Skrænterne Formation, but in terms of major elements the Group 1 tholeiites tend to have higher SiO_2 at a given $TiO_2/FeO(t)$ value than Skrænterne Formation lavas (Fig. 11b: Hansen *et al.*, 2002). The volumetrically minor Group 2 flows have higher La/Sm_N than most Milne Land Formation lavas and higher Dy/Yb_N than the Geikie Plateau Formation lavas. Although they have similar La/Sm_N and Dy/Yb_N to the Rømer Fjord Formation lavas, they can be distinguished from these lavas by their higher SiO_2 at a given $TiO_2/FeO(t)$ and higher Zr/Y. It is possible that the Group 2 flows represent a minor compositional variant with the Milne Land or Geikie Plateau Formation that is not seen in the Sortebræ profile.

Thus, it appears that alkalic magmatism in the Prinsen af Wales Bjerge region initiated during the eruption of the early–middle part of the plateau basalts (upper Milne Land or Geikie Plateau Formations). This is consistent with the 55 Ma age obtained from the vent 1 sample. This activity lasted until after the plateau basalt eruptions had ceased (53 Ma age from 'Lindsay Nunatak'), a total duration of at least 2 Myr. Additional evidence for alkalic magmatism contemporaneous with the upper two

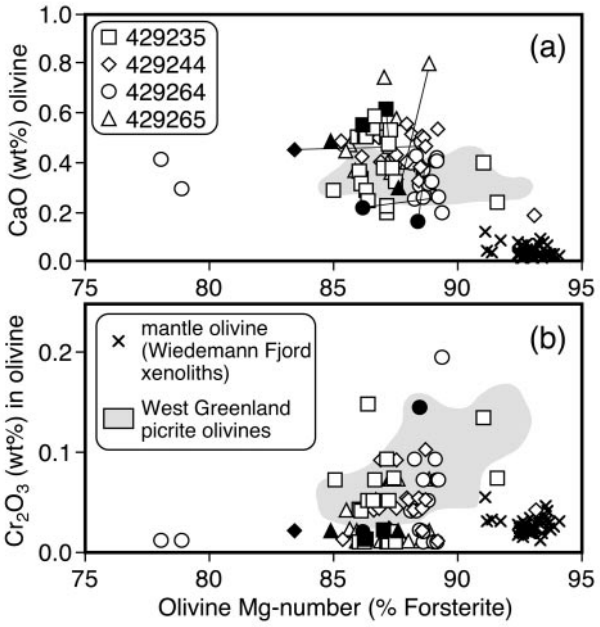

Fig. 10. Mg-number (% forsterite) vs (a) CaO and (b) Cr_2O_3, to illustrate the compositional range and affinity of olivines from the Prinsen af Wales Bjerge Formation lavas. Filled symbols represent rim compositions, with tie-lines to the adjacent core composition shown in (a). For comparison, olivines from West Greenland picrites (~61 Ma: Larsen & Pedersen, 2000) and from lithospheric mantle xenoliths (Wiedemann Fjord, East Greenland: Bernstein *et al.*, 1998*a*) are also plotted. Olivine Mg-number is atomic Mg/(Mg + Fe). Olivines were analysed at the Geological Institute, University of Copenhagen, using a JEOL733 electron microprobe (operating conditions: 15 kV accelerating voltage, 15 nA beam current, wavelength-dispersive analysis).

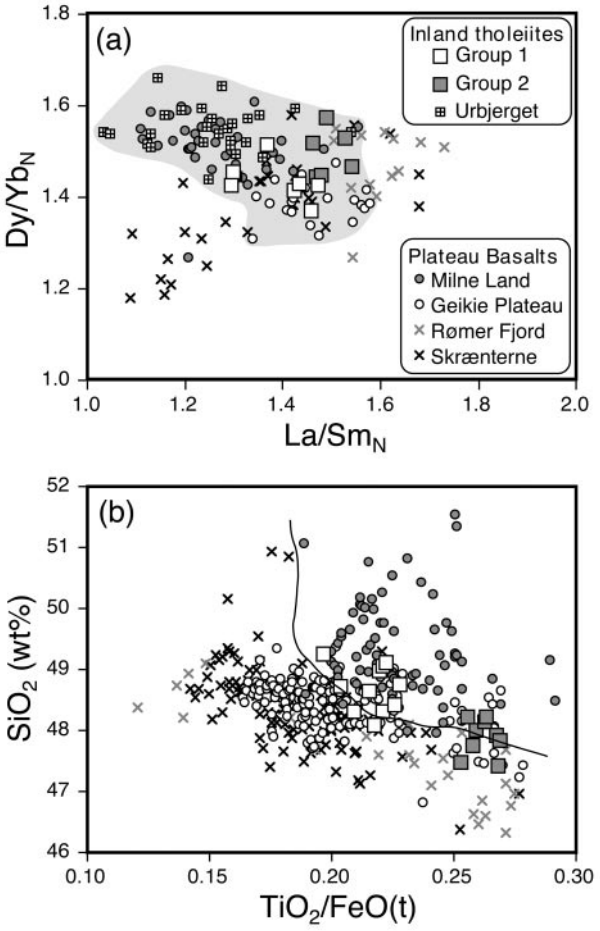

Fig. 11. (a) La/Sm_N vs Dy/Yb_N, (b) $TiO_2/FeO(t)$ vs SiO_2. Comparison of Prinsen af Wales Bjerge region tholeiites with the various formations recognized within the coastal plateau basalts: it should be noted that the formations are defined primarily by field characteristics and stratigraphy, rather than on compositional grounds. Data sources: plateau basalts (Larsen *et al.*, 1989; Tegner *et al.*, 1998*b*); Urbjerget lavas (Hansen *et al.*, 2002). The shaded field in (a) encloses analyses from the lower part of the plateau basalts (Milne Land and Geikie Plateau Formations, plus the inland Urbjerget tholeiites). The line in (b) marks the maximum SiO_2 content for a given TiO_2/FeO value seen in the upper part of the plateau basalts (Rømer Fjord and Skrænterne Formations).

formations of the tholeiitic plateau basalts comes from nephelinitic tuffs found interbedded within the Rømer Fjord Formation lavas (Larsen *et al.*, 1989), and a phonolitic tuff within the Skrænterne Formation lavas that is inferred to have been erupted from the Gardiner complex at 54 Ma (Fig. 1: Heister *et al.*, 2001). Furthermore, whereas the full stratigraphic sequence of the plateau basalts is preserved in the inland area near Gronau West (Fig. 1: Heister *et al.*, 2001), only lavas of the lower formations appear to have reached the Prinsen af Wales Bjerge region to the east.

The role of crustal assimilation

Magmas traversing the continental crust have the potential to modify their compositions by assimilating crustal material. The effects of crustal contamination on lava compositions in East and SE Greenland are most readily apparent in Pb isotope compositions because the local basement has a distinctive, very unradiogenic $^{206}Pb/^{204}Pb$ isotope composition (Leeman *et al.*, 1976; Taylor *et al.*, 1992; Kalsbeek *et al.*, 1993). Many of the Lower Basalts (Holm, 1988; Fram & Lesher, 1997; Hansen & Nielsen, 1999) and the offshore lavas drilled by the Ocean Drilling Program off SE Greenland (Fitton *et al.*, 1998, 2000; Saunders *et al.*, 1999) show clear evidence for significant contamination by such crustal material (Fig. 7). In detail, two compositionally distinct crustal contaminants affecting lavas in both regions can be recognized, distinguished primarily by differences in Sr isotopes (amphibolitic gneiss with relatively high $^{87}Sr/^{86}Sr$, and granulitic gneiss with relatively low $^{87}Sr/^{86}Sr$) but both with relatively unradiogenic $^{206}Pb/^{204}Pb$ and low εNd_i. From the Pb isotope variations (Fig. 7), it is clear that the extent of crustal

assimilation is, in general, lower in the plateau basalts than in the earlier Lower Basalts, and this limited crustal influence is also seen in the main group of tholeiitic lavas from the Prinsen af Wales Bjerge profiles. In contrast, the younger 'Lindsay Nunatak' tholeiites appear to be highly contaminated, as is evident from their unradiogenic $^{206}Pb/^{204}Pb$ of 14·9–16·2.

The Sr–Nd–Pb isotope data indicate a strong crustal influence in the Prinsen af Wales Bjerge alkalic lavas and also that the crustal assimilant is broadly similar in composition to that involved in the plateau basalts, Lower Basalts, and the early phase lavas drilled offshore further south. The relatively high $^{87}Sr/^{86}Sr$ of the inferred contaminant suggests dominance of amphibolitic rather than granulitic crustal material. The effects of crustal assimilation are also clear from the major and trace element data: the Si-enriched group have lower εNd_i and $^{206}Pb/^{204}Pb$ than the main group, and tend to have high Ba/La, K/Nb and U/Pb ratios, and lower Ce/Pb and Dy/Yb_N ratios, indicative of a higher proportion of assimilated Si-rich crust. The highest $^{187}Os/^{188}Os$ values (0·130–0·132) are found in the samples with the lowest εNd_i and $^{206}Pb/^{204}Pb$. This is consistent with addition of ancient crustal material with time-integrated elevated Re/Os and low Sm/Nd and U/Pb ratios, as is illustrated by one example of a plausible mixing curve (curve 1 in Fig. 8b). The question, though, is whether the main group are themselves slightly contaminated. Mixing arrays on Pb–Pb isotope diagrams are linear, and it is interesting that extrapolation of the alkalic lava trend on the $^{207}Pb/^{204}Pb$ vs $^{206}Pb/^{204}Pb$ (Fig. 7b) to higher $^{206}Pb/^{204}Pb$ (i.e. potentially less-contaminated compositions) intersects the trend of uncontaminated plateau basalt lavas and Icelandic basalts at $^{206}Pb/^{204}Pb$ values of 19·2–19·8. This is a plausible source composition for the Prinsen af Wales Bjerge lavas, and also explains their low $^{207}Pb/^{204}Pb$ relative to the plateau basalt samples. If we assume that this intersection point represents the Pb isotope composition of the uncontaminated magma, estimates for the amounts of contamination required to explain the lava data can be made using plausible compositions for the assimilated crustal material. These amounts depend on the choice of elemental and isotopic compositions assumed for the crustal end-member. If we take reasonable values as used in other studies of East Greenland magmatism (e.g. Blichert-Toft *et al.*, 1992; Hansen & Nielsen, 1999; Saunders *et al.*, 1999), then the main group of alkalic lavas can be explained by ~4% assimilation whereas the most contaminated samples require ~15–20% assimilation. The differences in SiO_2 between the main group and the high-Si group are also consistent with such amounts of assimilation.

Thus, rather surprisingly, there is clear evidence for greater extents of crustal assimilation in the alkalic lavas, despite their elevated trace element contents, than in the associated underlying tholeiitic lavas. This marked crustal influence in the Prinsen af Wales Bjerge alkalic lavas, together with the absence of mantle xenoliths, is suggestive of small magma batches that stalled in the crust *en route* to the surface. The high levels of contamination compared with the relatively uncontaminated tholeiitic plateau basalts provide further evidence that the Prinsen af Wales Bjerge alkalic lavas, and the younger tholeiites on 'Lindsay Nunatak', are locally erupted through newly established magma conduits, whereas the voluminous plateau basalt lavas probably flowed into the region fed from long-lived plumbing systems nearer the coast or from the east (Pedersen *et al.*, 1997). Possible eruption vent sites for the Prinsen af Wales Bjerge alkalic lavas have been identified in the '1982 Nunatak', 'Tjeldebjerge', Trillingerne, and Spring Journey Nunataks regions (Fig. 1: Wager, 1947; Brown *et al.*, 2000; Hansen *et al.*, 2002). The scatter of the data on the various isotope plots (Figs 7 and 8) rules out a single contamination trend, consistent with frequent small magma batches traversing the crust and stalling at different levels at different times.

Mantle source for 'uncontaminated' Prinsen af Wales Bjerge alkalic lavas

As discussed above, none of the Prinsen af Wales Bjerge Formation samples represent pristine uncontaminated mantle-derived magmas. From the three least contaminated samples (429244, 429265, 429272) and the contamination model calculations, an 'uncontaminated' magma is inferred to have the following distinctive isotopic characteristics: $^{87}Sr/^{86}Sr_i \sim 0{\cdot}7035$, $\varepsilon Nd_i \sim +5$ to $+6$, $\varepsilon Hf_i \sim +8$ to $+9$, $^{206}Pb/^{204}Pb_i \sim 19{\cdot}2$–$19{\cdot}8$, $^{187}Os/^{188}Os_i \sim 0{\cdot}120$–$0{\cdot}126$, and $^{3}He/^{4}He > 18\ R/R_A$. These Sr–Nd–Pb isotope characteristics are broadly similar to the 'high ^{206}Pb plume component' that contributed to the 56–54 Ma tholeiitic dykes on the Faeroes (Holm *et al.*, 2001), and the '^{206}Pb-rich, p component' that Hanan & Schilling (1997) inferred to be representative of the main Icelandic plume mantle.

The primitive-mantle-normalized diagram (Fig. 5a) shows relatively smooth trace element patterns, except for slight negative anomalies at K and P, with normalized abundances reaching maxima at Nb and Ta. The strongly fractionated HREE patterns (Dy/Yb_N 2·1–2·7) indicate melting in the presence of residual garnet. These magmas share many trace element characteristics with HIMU ocean island basalt (OIB) magmas (Fig. 5b: e.g. Sun & McDonough, 1989; Weaver, 1991; Hofmann, 1997), namely low La/Nb (0·7–0·8), K/Nb (<180), Th/Nb (<0·08) and Ba/La (5–8), but without the extreme $^{206}Pb/^{204}Pb$ (>20) values found in typical HIMU OIB such as St. Helena. Thirlwall (1997) refers to other OIB magmas with similar characteristics as being derived from 'young

HIMU' mantle; i.e. mantle modified to give similar trace element features to the extreme HIMU source, but sufficiently recently so as not to have allowed in-growth of radiogenic ^{206}Pb. The positive primitive-mantle-normalized anomaly of Nb relative to La, Th, Ba and K in the HIMU OIB source is usually attributed to a contribution from recycled subduction-processed residual ocean slab material.

The 'Lindsay Nunatak' nephelinite is compositionally distinct from the Prinsen af Wales Bjerge Formation lavas (i.e. contrasting primitive-mantle-normalized trace element patterns in Fig. 5, and markedly different Pb isotope compositions). These differences are indicative of a different petrogenetic origin. It has trace element features consistent with small-degree melting in the presence of minor residual phases that hold back elements such as K, Sr, Pb and P. The Pb isotope data and U–Th–Pb abundances for this sample are consistent with being derived from a source broadly similar to that of the Palaeogene tholeiitic and alkalic lavas but that had elevated U/Pb and Th/Pb ratios for the last ~400–800 Myr. Thus it is plausible that this nephelinite, as well as the contemporaneous Gardiner intrusion, represents melts of local lithospheric mantle that was metasomatized during the Caledonian orogeny.

Recycled components in Iceland plume-related magmatism

Recycled components are increasingly invoked to explain much of the isotopic variations seen within OIB globally (e.g. Weaver, 1991; Hofmann, 1997). It has been proposed that the compositional variations in Icelandic and Hawaiian lavas can be explained by melting of different components that make up a complete section of recycled subducted slab (e.g. Lassiter & Hauri, 1998; Chauvel & Hémond, 2000). The low-εNd component (alkalic basalts, Iceland; 'Koolau' component, Hawaii) is interpreted as the upper part of recycled oceanic crust (basalt ± pelagic sediment), whereas the high-εNd component (depleted picritic lavas, Iceland; 'Kea' component, Hawaii) is interpreted as the gabbroic part of the recycled slab. The role for DMM (depleted MORB mantle) as a magma source at both places appears to be minimal (e.g. Lassiter & Hauri, 1998; Chauvel & Hémond, 2000), and the high $^{3}He/^{4}He$ signal is inferred to be primarily from the plume mantle hosting the recycled slabs (e.g. Eiler *et al.*, 1998; Hilton *et al.*, 1999).

In this paper, we are concerned primarily with the nature of the 'enriched' low-εNd component(s). It is not clear if more than one 'enriched' component is required to explain the compositional variety of trace element enriched, low-εNd magmas found throughout the North Atlantic region, and also how the Prinsen af Wales Bjerge alkalic lavas compare compositionally with these other magmatic suites. Examples include alkalic Iceland lavas (e.g. Hards *et al.*, 1995; Chauvel & Hémond, 2000; Prestvik *et al.*, 2001), Jan Mayen lavas (Schilling *et al.*, 1999; Trønnes *et al.*, 1999), Vestbrona nephelinites, offshore Norway (56 Ma: Prestvik *et al.*, 1999) and Palaeogene melilitites, NE Greenland (Bernstein *et al.*, 2000). Trønnes *et al.* (1999) have argued, for example, that the compositional features of Jan Mayen alkaline lavas can be explained by contributions from Nb-rich melts derived from a recycled oceanic crust component.

The highly alkaline ultrabasic lavas found in the Nunatak Region of NE Greenland are the most compositionally extreme of all the Palaeogene alkaline rocks in East Greenland (Bernstein *et al.*, 2000), and they are similar in composition to the meymechites associated with the Siberian flood basalts (Horan *et al.*, 1995). Bernstein *et al.* (2000, 2001) suggested that these rocks represent low-degree melting at high pressures (>5 GPa) of subducted oceanic lithosphere material within the Iceland plume and also that variable mixing of such a component with a depleted MORB-like melt can explain the main compositional features of the plateau basalts. The primitive-mantle-normalized trace element pattern of such a melilitite is broadly similar to that of the main group of Prinsen af Wales Bjerge alkalic lavas, although the melilitite has higher incompatible trace element abundances and higher La/Yb and Dy/Yb (Fig. 5b). The Nunatak Region lavas have lower SiO_2 and Al_2O_3, and higher Fe_2O_3 and TiO_2 (Fig. 4), which, together with their higher Dy/Yb, suggests low-degree melting at higher pressures than for the Prinsen af Wales Bjerge alkalic lavas, perhaps beneath a thicker lithospheric cap. Isotope data are needed to test the possible similarity of mantle sources between the Nunatak Region melilitites and the Prinsen af Wales Bjerge alkalic lavas, although the few Sr and Nd isotope data of Bernstein *et al.* (2001) are broadly consistent with such a model. Furthermore, the $^{206}Pb/^{204}Pb$ value (>19·2) inferred for an uncontaminated Prinsen af Wales Bjerge magma is sufficiently radiogenic to represent the 'enriched' component that is required to explain the isotopic variations within the plateau basalts (Peate & Stecher, 2002).

Compositional similarities between alkalic magmas from Jan Mayen, Iceland and Vestbrona (e.g. Fig. 12) led Trønnes *et al.* (1999) to suggest a common 'enriched', low-εNd mantle component with low $^{3}He/^{4}He$ (Schilling *et al.*, 1999) that was present within the ancestral Iceland plume and that is now widely dispersed throughout the North Atlantic upper mantle. However, the Prinsen af Wales Bjerge alkalic lavas and the Nunatak Region lavas are markedly different in composition from this component, both having lower Ba/La and higher Zr/Nb (Fig. 12). This implies that the ancestral Iceland

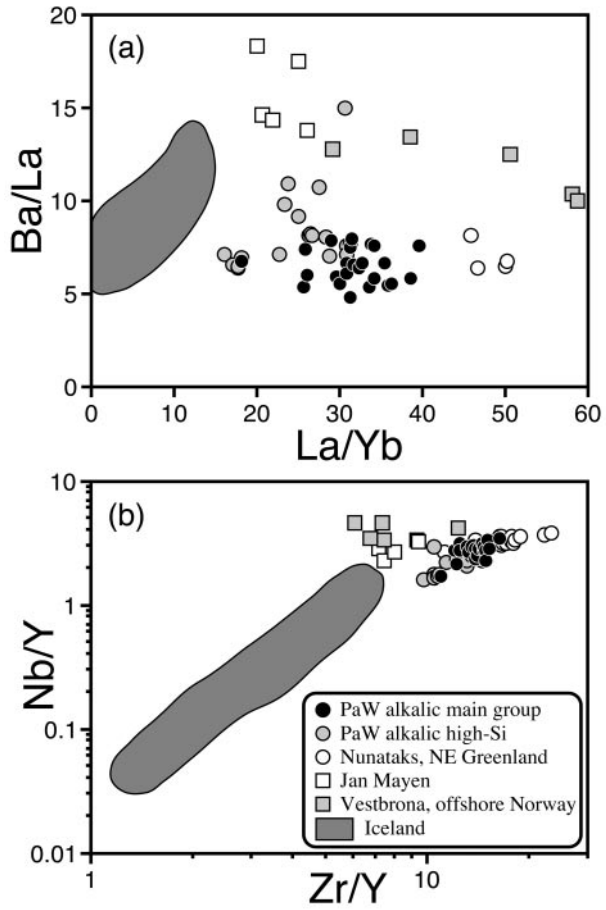

Fig. 12. (a) La/Yb vs Ba/La, (b) Zr/Y vs Nb/Y (Fitton *et al.*, 1997), to compare the Prinsen af Wales Bjerge alkalic lavas with Nunatak Region lavas (Bernstein *et al.*, 2000, 2001), Jan Mayen (Trønnes *et al.*, 1999), Vestbrona nephelinites (56 Ma, offshore Norway: Prestvik *et al.*, 1999) and Icelandic basalts (Hémond *et al.*, 1993; Hards *et al.*, 1995; Hardarson *et al.*, 1997; Stecher *et al.*, 1999; Chauvel & Hémond, 2000; Skovgaard *et al.*, 2001; and references therein).

plume contained more than one 'enriched', low-εNd component, as suggested by Hanan & Schilling (1997).

At the time of the Prinsen af Wales Bjerge alkalic magmatism, the Iceland plume stem is inferred to have been beneath thick Greenland cratonic lithosphere, within 200–300 km of the Prinsen af Wales Bjerge region (Lawver & Müller, 1994; Torsvik *et al.*, 2001). Melting beneath the inland regions was largely restricted to the enriched recycled slab components (see also Bernstein *et al.*, 2000, 2001) because the thick lithospheric cap prevented the plume mantle from upwelling to depths shallow enough for melting to occur above its dry solidus (~115 km: Ito *et al.*, 1999). At deeper levels, perhaps up to 180–210 km (Ito *et al.*, 1999), incipient 'wet' melting caused by dehydration and defluidization of the upwelling plume mantle will have produced fluids that were probably highly mobile and capable of transporting significant amounts of helium plus other rare gases and volatiles (e.g. Schilling *et al.*, 1999; Breddam *et al.*, 2000). Thus, one model to explain the high $^{3}He/^{4}He$ ratios measured in the Prinsen af Wales Bjerge Formation lavas is addition of Iceland plume-derived helium from such deep He-rich fluids to melts of the enriched recycled slab components.

Hf and Os isotope constraints on the nature of the recycled component(s)

Isotope data on the least contaminated Prinsen af Wales Bjerge alkalic lavas can provide some constraints on the nature of the recycled low-εNd component. For example, ancient pelagic sediments have unradiogenic Nd and Hf isotope compositions that plot above the 'mantle array' in Fig. 8a (i.e. they have more radiogenic εHf than normal OIB for a given εNd value). The shallow slope of the Hawaiian data trend and relatively high εHf of the low-εNd 'Koolau' component indicate the presence of old recycled pelagic sediment in this mantle source (Blichert-Toft *et al.*, 1999). This contrasts with the steep slope of the Icelandic data trend, relative to the 'mantle array'. The inferred composition of the uncontaminated Prinsen af Wales Bjerge magma lies on an extension of this data trend below the 'mantle array', limiting the role of pelagic sedimentary material in this component. Nd and Hf isotope data on HIMU OIB lavas plot in a similar position to the Prinsen af Wales Bjerge lavas, below the 'mantle array', and Salters & White (1998) demonstrated that this is consistent with derivation primarily from an old recycled oceanic crust component. Blichert-Toft & Albarède (1997) explained such characteristics by re-melting ancient residues produced by garnet-absent melting.

The compatibility of Os and moderate incompatibility of Re during melting produces high Re/Os and, with time, high $^{187}Os/^{188}Os$ in mafic melts, whereas the peridotitic mantle residue will have low Re/Os, eventually leading to low $^{187}Os/^{188}Os$. Thus, ancient recycled mafic components in OIB can be identified from their elevated $^{187}Os/^{188}Os$ values as seen, for example in HIMU OIB lavas ($^{187}Os/^{188}Os$ ~0·155: Hauri & Hart, 1993; Shirey & Walker, 1998). However, the Prinsen af Wales Bjerge alkalic lavas have sub-chondritic Os isotope compositions ($^{187}Os/^{188}Os_i$ 0·120–0·126; γOs_i −7 to −2), indicating a peridotitic rather than pyroxenitic source. There are several possibilities to consider:

(1) melting of a DMM source, which has suitably low $^{187}Os/^{188}Os$ ratios of 0·123–0·128 (defined by abyssal peridotites and the least radiogenic MORB samples: Shirey & Walker, 1998). However, this can be ruled out as it has significantly higher εNd than the Prinsen af Wales Bjerge lavas (~+10 vs ~+4).

(2) Another possible source is sub-continental lithospheric mantle. This is often characterized by sub-chondritic Os isotope values reflecting ancient melt-related Re depletion (average $^{187}Os/^{188}Os = 0{\cdot}113$: Shirey & Walker, 1998), and data on the Wiedemann Fjord xenoliths show that such depleted lithospheric mantle occurs beneath East Greenland ($^{187}Os/^{188}Os_m$ 0·101–0·126: Hanghøj *et al.*, 2001). The very low $^{187}Os/^{188}Os_i$ (0·112–0·121: Carlson *et al.*, 1996) of some mafic potassic magmas in central Brazil demonstrates that alkalic magmas can result from low-degree melting of lithospheric mantle, rather than the underlying asthenospheric or plume mantle. However, it is difficult to reconcile the elevated $^3He/^4He$ ratios of the Prinsen af Wales Bjerge alkaline lavas with an origin purely from melting of continental lithospheric mantle, as such mantle is generally characterized by $^3He/^4He$ ratios similar to, or lower than, MORB (e.g. Dunai & Baur, 1995).

(3) Assimilation of lithospheric mantle material by an 'enriched' plume-derived melt, as suggested for high-MgO meymechites from Siberia (Horan *et al.*, 1995), would rapidly decrease the Os isotope composition of the melt with little effect on other radiogenic isotope systems (Sr–Nd–Pb–Hf) owing to the marked contrast between the Os and Sr–Nd–Pb–Hf contents in the two end-members. The 'enriched' plume component seen in early phase magmatism in West Greenland and Baffin Island (Schaefer *et al.*, 2000; A. J. R. Kent, unpublished data, 2001) provides a suitable end-member to test this mixing model for the Prinsen af Wales Bjerge alkalic lavas. It has similar εNd_i ($\sim +5$) to the 'uncontaminated' Prinsen af Wales Bjerge magma, but with higher γOs_i ($\sim +5$ vs -5). The Prinsen af Wales Bjerge data can be modelled by addition of 15–25% of a lithospheric mantle component (curve 2 in Fig. 8b). Although such a model cannot be excluded, several lines of evidence suggest that this might not be the origin of the observed sub-chondritic Os isotope compositions. First, there is no clear evidence for any xenocrystic lithospheric mantle olivines in the samples, and, second, analyses of Holocene alkalic basalts from Iceland (Smit *et al.*, 2001) show that material with relatively low εNd_i ($\sim +5$) and sub-chondritic γOs_i (~ -2) is indeed present within the upwelling Iceland plume.

One way of reconciling the Os isotope data with a slab recycling model is if the Os is primarily contributed by the mantle section of the recycled oceanic lithosphere, in contrast to the incompatible elements that are derived principally from either the basaltic portion of the recycled crust (e.g. Lassiter & Hauri, 1998; Chauvel & Hémond, 2000) or metasomatic veins within the mantle section (e.g. Niu *et al.*, 2002). Chauvel & Hémond (2000) similarly argued that a contribution from melting of the harzburgitic part of old recycled oceanic lithosphere was necessary to account for the high Mg and Ni contents of Icelandic basalts.

CONCLUSIONS

(1) Stratigraphic, compositional and ^{40}Ar–^{39}Ar age data suggest that alkalic magmatism in the inland Prinsen af Wales Bjerge was contemporaneous with the eruption of the upper parts of the voluminous tholeiitic plateau basalt flood volcanism (56–54 Ma) in East Greenland. This alkalic activity, however, persisted after the plateau basalt eruptions had ceased, as indicated by field relations and a new ^{40}Ar–^{39}Ar age of 53 Ma.

(2) The Prinsen af Wales Bjerge alkaline lavas show a marked crustal influence, more so than the underlying tholeiitic lavas. This suggests the establishment of new local magmatic plumbing systems inland, distinct from the long-lived ones nearer the coast that fed the voluminous tholeiitic plateau basalt eruptions.

(3) The mantle source for the Prinsen af Wales Bjerge alkalic lavas was characterized by elevated $^3He/^4He$ (>18 R/R_A), sub-chondritic Os isotope composition ($^{187}Os/^{188}Os_i$ 0·120–0·126), radiogenic $^{206}Pb/^{204}Pb$ (19·2–19·8), low εNd_i ($\sim +5$ to $+6$) and εHf_i ($\sim +8$ to $+9$) that plot below the 'Nd–Hf mantle array', and trace element characteristics broadly similar to HIMU OIB, with low K/Nb, Ba/La and La/Nb.

(4) Although the East Greenland lithospheric mantle is characterized by sub-chondritic Os isotope values, it is not straightforward to account for the overall compositional features of the Prinsen af Wales Bjerge alkalic magmas by the participation of such mantle.

(5) A source primarily of recycled material within the upwelling Iceland plume mantle is preferred, although some minor assimilation of lithospheric mantle material cannot be ruled out. One plausible model to explain the compositional features of the Prinsen af Wales Bjerge alkalic magmas is preferential melting of recycled material within the plume upwelling beneath the thick lithospheric cap, with ^3He contributed from volatile-rich fluids from the plume. Although the exact nature of this recycled component is not yet resolved, Hf isotopes rule out any significant role for recycled pelagic sediment and the inferred low $^{187}Os/^{188}Os$ limits the participation of recycled basaltic material and argues instead for a contribution from the mantle section of the recycled slab.

ACKNOWLEDGEMENTS

We thank Tod Waight for analytical assistance, Robert Frei for help with the Os analyses and for access to the Geological Institute, University of Copenhagen, chemistry laboratories, Philippe Telouk for help with the

Plasma 54 at Lyon, Ole Stecher for processing the ICP-MS trace element data, Phil Neuhoff for assistance in sampling the lava profiles in 1995, and Troels Nielsen for organizing the field logistics in 1995 and 2000 and for numerous discussions. Comments on an earlier version by Lotte Melchoir Larsen and Stefan Bernstein, and journal reviews by Ian Parkinson, Rob Ellam and Godfrey Fitton are appreciated. Thanks also go to the SWIFT cruise participants on the R.V. *Marion Dufresne* for providing a stimulating environment in the middle of the Indian Ocean, where the first manuscript draft was largely written. This study was funded by the Danish National Research Foundation. J.B.T. acknowledges financial support from the Institut National des Sciences de l'Univers. Geochronological facilities at Oregon State University are supported by the National Science Foundation (USA).

REFERENCES

Anwar, Y. M. (1955). Geological investigations in East Greenland: part V, The petrography of the Prinsen af Wales Bjerge lavas. *Meddelelser om Grønland* **135**, 1–31.

Bennett, V. C., Esat, T. M. & Norman, M. D. (1996). Two mantle-plume components in Hawaiian picrites inferred from correlated Os–Pb isotopes. *Nature* **381**, 221–224.

Bernstein, S., Kelemen, P. B. & Brooks, C. B. (1998*a*). Depleted spinel harzburgite xenoliths in Tertiary dykes from East Greenland: restites from high-degree melting. *Earth and Planetary Science Letters* **154**, 221–235.

Bernstein, S., Kelemen, P. B., Tegner, C., Kurz, M. D., Blusztajn, J. & Brooks, C. K. (1998*b*). Post-breakup basaltic magmatism along the East Greenland Tertiary rifted margin. *Earth and Planetary Science Letters* **160**, 845–862.

Bernstein, S., Leslie, A. G., Higgins, A. K. & Brooks, C. K. (2000). Tertiary alkaline volcanics in the Nunatak Region, Northeast Greenland: new observations and comparison with Siberian maymechites. *Lithos* **53**, 1–20.

Bernstein, S., Brooks, C. K. & Stecher, O. (2001). Enriched component of the proto-Icelandic mantle plume revealed in alkaline Tertiary lavas from East Greenland. *Geology* **29**, 859–862.

Blichert-Toft, J. (2001). On the Lu–Hf isotope geochemistry of silicate rocks. *Geostandards Newsletter* **25**, 41–56.

Blichert-Toft, J. & Albarède, F. (1997). The Lu–Hf isotope geochemistry of chondrites and the evolution of the mantle–crust system. *Earth and Planetary Science Letters* **148**, 243–258.

Blichert-Toft, J., Lesher, C. E. & Rosing, M. T. (1992). Selectively contaminated magmas of the Tertiary East Greenland macrodike complex. *Contributions to Mineralogy and Petrology* **110**, 154–172.

Blichert-Toft, J., Chauvel, C. & Albarède, F. (1997). Separation of Hf and Lu for high-precision isotope analysis of rock samples by magnetic sector multiple collector ICP-MS. *Contributions to Mineralogy and Petrology* **127**, 248–260.

Blichert-Toft, J., Frey, F. A. & Albarède, F. (1999). Hf isotope evidence for pelagic sediments in the source of Hawaiian basalts. *Science* **285**, 879–882.

Breddam, K., Kurz, M. D. & Storey, M. (2000). Mapping out the conduit of the Iceland mantle plume with helium isotopes. *Earth and Planetary Science Letters* **176**, 45–55.

Brooks, C. K. & Rucklidge, J. C. (1974). Strongly undersaturated Tertiary volcanic rocks from the Kangerdlugsuuaq area, East Greenland. *Lithos* **7**, 239–248.

Brooks, C. K., Fawcett, J. J. & Gittins, J. (1976). Caledonian magmatic activity in south-eastern Greenland. *Nature* **260**, 694–696.

Brown, P. E., Evans, I. B. & Becker, S. M. (1996). The Prince of Wales Formation—post-flood basalt alkali volcanism in the Tertiary of East Greenland. *Contributions to Mineralogy and Petrology* **123**, 424–434.

Brown, P. E., Evans, I. B. & Becker, S. M. (2000). Alkaline basaltic magmatism in the Tertiary of central East Greenland—the Trekantnunatakker. *Transactions of the Royal Society of Edinburgh: Earth Sciences* **90**, 165–172.

Carlson, R. W., Esperança, S. & Svisero, D. (1996). Chemical and Os isotopic study of Cretaceous potassic rocks from southern Brazil. *Contributions to Mineralogy and Petrology* **125**, 393–405.

Chaffey, D. J., Cliff, R. A. & Wilson, B. M. (1989). Characterisation of the St Helena magma source. In: Saunders, A. D. & Norry, M. J. (eds) *Magmatism in the Ocean Basins. Geological Society, London, Special Publications* **42**, 257–276.

Chauvel, C. & Hémond, C. (2000). Melting of a complete section of recycled oceanic crust: trace element and Pb isotopic evidence from Iceland. *Geochemistry, Geophysics, Geosystems* **1**, paper number 1999GC000002.

Condomines, M., Grönvold, K., Hooker, P. J., Muehlenbachs, K., O'Nions, R. K., Oskarsson, N. & Oxburgh, E. R. (1983). Helium, oxygen, strontium and neodymium isotopic relationships in Icelandic volcanics. *Earth and Planetary Science Letters* **66**, 125–136.

Dunai, T. J. & Baur, H. (1995). Helium, neon, and argon systematics of the European subcontinental mantle: implications for its geochemical evolution. *Geochimica et Cosmochimica Acta* **59**, 2767–2783.

Eiler, J. M., Farley, K. A. & Stolper, E. M. (1998). Correlated helium and lead isotope variations in Hawaiian lavas. *Geochimica et Cosmochimica Acta* **62**, 1977–1984.

Ellam, R. M. & Stuart, F. M. (2000). The sub-lithospheric source of North Atlantic basalts: evidence for, and significance of, a common end-member. *Journal of Petrology* **41**, 919–932.

Farley, K. A. & Neroda, E. (1998). Noble gases in the Earth's mantle. *Annual Review of Earth and Planetary Sciences* **26**, 189–218.

Fawcett, J. J., Gittins, J., Rucklidge, J. C. & Brooks, C. K. (1982). Petrology of Tertiary lavas from the western Kangerdlugssuaq area, East Greenland. *Mineralogical Magazine* **45**, 211–218.

Fitton, J. G., Saunders, A. D., Norry, M. J., Hardarson, B. S. & Taylor, R. N. (1997). Thermal and chemical structure of the Iceland plume. *Earth and Planetary Science Letters* **153**, 197–208.

Fitton, J. G., Hardarson, B. S., Ellam, R. M. & Rogers, G. (1998). Sr-, Nd-, and Pb-isotopic composition of volcanic rocks from the southeast Greenland margin at 63°N: temporal variation in crustal contamination during continental breakup. In: Saunders, A. D., Larsen, H. C. & Wise, S. W. (eds) *Proceedings of the Ocean Drilling Program, Scientific Results, 152*. College Station, TX: Ocean Drilling Program, pp. 351–357.

Fitton, J. G., Larsen, L. M., Saunders, A. D., Hardarson, B. S. & Kempton, P. D. (2000). Palaeogene continental to oceanic magmatism on the SE Greenland continental margin at 63°N: a review of the results of Ocean Drilling Program Legs 152 and 163. *Journal of Petrology* **38**, 231–275.

Fram, M. S. & Lesher, C. E. (1997). Generation and polybaric differentiation of East Greenland early Tertiary flood basalts. *Journal of Petrology* **38**, 231–275.

Graham, D. W., Larsen, L. M., Hanan, B. B., Storey, M., Pedersen, A. K. & Lupton, J. E. (1998). Helium isotope composition of the

early Iceland mantle plume inferred from the Tertiary picrites of West Greenland. *Earth and Planetary Science Letters* **160**, 241–255.

Gurenko, A. A., Hansteen, T. H. & Schmincke, H.-U. (1996). Evolution of parental magmas of Miocene shield basalts of Gran Canaria (Canary Islands): constraints from crystal, melt and fluid inclusions in minerals. *Contributions to Mineralogy and Petrology* **124**, 422–435.

Hanan, B. B. & Schilling, J.-G. (1997). The dynamic evolution of the Iceland mantle plume: the Pb isotope perspective. *Earth and Planetary Science Letters* **151**, 43–60.

Hanan, B. B., Blichert-Toft, J., Kingsley, R. & Schilling, J.-G. (2000). Depleted Iceland mantle plume geochemical signature: artifact of multicomponent mixing? *Geochemistry, Geophysics, Geosystems* **1**, paper number 1999GC000009.

Hanghøj, K., Kelemen, P., Bernstein, S., Blusztajn, J. & Frei, R. (2001). Osmium isotopes in the Wiedemann Fjord mantle xenoliths: a unique record of cratonic mantle formation by melt depletion in the Archaean. *Geochemistry, Geophysics, Geosystems* **2**, paper number 2000GC000085.

Hansen, H. & Nielsen, T. F. D. (1999). Crustal contamination in Palaeogene East Greenland flood basalts: plumbing system evolution during continental rifting. *Chemical Geology* **157**, 89–118.

Hansen, H., Pedersen, A. K., Duncan, R. A., Bird, D. K., Brooks, C. K., Fawcett, J. J., Gittins, J., Gorton, M. & O'Day, P. (2002). Volcanic stratigraphy of the southern Prinsen af Wales Bjerge region, East Greenland. In: Jolley, D. W. & Bell, B. R. (eds) *The North Atlantic Igneous Province: Stratigraphy, Tectonics, Volcanic and Magmatic Processes. Geological Society, London, Special Publications* **197** (in press).

Hardarson, B. S., Fitton, J. G., Ellam, R. M. & Pringle, M. S. (1997). Rift relocation—a geochemical and geochronological investigation of a palaeo-rift in northwest Iceland. *Earth and Planetary Science Letters* **153**, 181–196.

Hards, V. L., Kempton, P. D. & Thompson, R. N. (1995). The heterogeneous Iceland plume: new insights from the alkaline basalts of the Snaefell volcanic centre. *Journal of the Geological Society, London* **152**, 1003–1009.

Hauri, E. H. & Hart, S. R. (1993). Re–Os isotope systematics of HIMU and EMII oceanic island basalts from the south Pacific Ocean. *Earth and Planetary Science Letters* **114**, 353–371.

Heister, L. E., O'Day, P. A., Brooks, C. K., Neuhoff, P. S. & Bird, D. K. (2001). Pyroclastic deposits within the East Greenland Tertiary flood basalts. *Journal of the Geological Society, London* **158**, 269–284.

Hémond, C., Arndt, N. T., Lichtenstein, U. & Hofmann, A. W. (1993). The heterogeneous Iceland mantle plume: Nd–Sr–O isotopes and trace element constraints. *Journal of Geophysical Research* **98**, 15833–15850.

Hilton, D. R., Grönvold, K., Macpherson, C. G. & Castillo, P. R. (1999). Extreme $^{3}He/^{4}He$ ratios in northwest Iceland: constraining the common component in mantle plumes. *Earth and Planetary Science Letters* **173**, 53–60.

Hofmann, A. W. (1997). Mantle geochemistry: the message from oceanic volcanism. *Nature* **385**, 219–229.

Hogg, A. J. (1985). The petrology and geochemistry of the Prinsen af Wales Bjerge, East Greenland. M.Sc. thesis, University of Toronto, pp. 1–99.

Hogg, A. J., Fawcett, J. J., Gittins, J. & Gorton, M. P. (1989). Cyclical variation in composition in continental tholeiites of East Greenland. *Canadian Journal of Earth Science* **26**, 534–543.

Holm, P. M. (1988). Nd, Sr and Pb isotope geochemistry of the Lower Lavas, E. Greenland Tertiary igneous province. In: Morton, A. C. & Parson, L. M. (eds) *Early Tertiary Volcanism and the Opening of the NE Atlantic. Geological Society, London, Special Publications* **49**, 181–195.

Holm, P. M., Hald, N. & Waagstein, R. (2001). Geochemical and Pb–Sr–Nd isotopic evidence for separate hot depleted and Iceland plume mantle sources for the Paleogene basalts of the Faroe Islands. *Chemical Geology* **178**, 95–125.

Horan, M. F., Walker, R. J., Fedorenko, V. A. & Czamanske, G. K. (1995). Osmium and neodymium isotopic constraints on the temporal and spatial evolution of Siberian flood basalt sources. *Geochimica et Cosmochimica Acta* **59**, 5159–5168.

Ito, G., Shen, Y., Hirth, G. & Wolfe, C. J. (1999). Mantle flow, melting, and dehydration of the Iceland mantle plume. *Earth and Planetary Science Letters* **165**, 81–96.

Kalsbeek, F., Austrheim, H., Bridgwater, D., Hansen, B. T., Pedersen, S. & Taylor, P. N. (1993). Geochronology of Archaean and Proterozoic events in the Ammassalik area, south-east Greenland, and comparisons with the Lewisian of Scotland and the Nagssugtoqidian of West Greenland. *Precambrian Research* **62**, 239–270.

Kempton, P. D., Fitton, J. G., Saunders, A. D., Nowell, G. M., Taylor, R. N., Hardarson, B. S. & Pearson, G. (2000). The Iceland plume in space and time: a Sr–Nd–Pb–Hf study of the North Atlantic rifted margin. *Earth and Planetary Science Letters* **177**, 255–271.

Kurz, M. D., Meyer, P. S. & Sigurdsson, H. (1985). Helium isotope systematics within the neovolcanic zones of Iceland. *Earth and Planetary Science Letters* **74**, 291–305.

Kystol, J. & Larsen, L. M. (1999). Analytical procedures in the rock geochemical laboratory of the Geological Survey of Denmark and Greenland. *Geology of Greenland Survey Bulletin* **184**, 59–62.

Larsen, L. M. & Pedersen, A. K. (2000). Processes in high-Mg, high-T magmas: evidence from olivine, chromite and glass in Palaeogene picrites from West Greenland. *Journal of Petrology* **41**, 1071–1098.

Larsen, L. M., Watt, W. S. & Watt, M. (1989). Geology and petrology of the Lower Tertiary plateau basalts of the Scoresby Sund region, East Greenland. *Bulletin Grønlands Geologiske Undersøgelse* **157**, 1–164.

Lassiter, J. C. & Hauri, E. H. (1998). Osmium isotope variations in Hawaiian lavas: evidence for recycled oceanic lithosphere in the Hawaiian plume. *Earth and Planetary Science Letters* **164**, 483–496.

Lawver, L. A. & Müller, R. D. (1994). Iceland hotspot track. *Geology* **22**, 311–314.

Le Bas, M. J. (2000). IUGS classification of the high-Mg and picritic volcanic rocks. *Journal of Petrology* **41**, 1467–1470.

Leeman, W. P., Dasch, E. J. & Kays, M. A. (1976). $^{207}Pb/^{204}Pb$ whole-rock age of gneisses from the Kangerdlugssuaq area, eastern Greenland. *Nature* **263**, 469–471.

Luais, B., Telouk, P. & Albarède, F. (1997). Precise and accurate neodymium isotopic measurements by plasma-source mass spectrometry. *Geochimica et Cosmochimica Acta* **61**, 4847–4854.

MacDonald, G. A. & Katsura, T. (1964). Chemical composition of Hawaiian lavas. *Journal of Petrology* **5**, 83–133.

Marty, B., Upton, B. G. J. & Ellam, R. M. (1998). Helium isotopes in early Tertiary basalts, northeast Greenland: evidence for 58 Ma plume activity in the North Atlantic–Iceland volcanic province. *Geology* **26**, 407–410.

McDonough, W. F. & Sun, S.-S. (1995). The composition of the Earth. *Chemical Geology* **120**, 223–253.

Meisel, T., Walker, R. J. & Morgan, J. W. (1996). The osmium isotopic composition of the Earth's primitive upper mantle. *Nature* **383**, 517–520.

Nägler, T. F. & Frei, R. (1997). 'Plug-in' Os distillation. *Schweizerische Mineralogische und Petrographische Mitteilungen* **77**, 123–127.

Nielsen, T. F. D. (1987). Tertiary alkaline magmatism in East Greenland: a review. In: Fitton, J. G. & Upton, B. J. G. (eds) *Alkaline Igneous Rocks. Geological Society, London, Special Publications* **30**, 489–515.

Nielsen, T. F. D. (1994). Alkaline dyke swarms of the Gardiner Complex and the origin of ultramafic alkaline complexes. *Geochemistry International* **31**, 37–56.

Nielsen, T. F. D., Soper, N. J., Brooks, C. K., Faller, A. M., Higgins, A. C. & Matthews, D. W. (1981). The pre-basaltic sediments and the lower lavas at Kangerdlugssuaq, East Greenland: their stratigraphy, lithology, palaeomagnetism and petrology. *Meddelelser om Grønland Geoscience* **6**, 1–25.

Niu, Y., Regelous, M., Wendt, I. J., Batiza, R. & O'Hara, M. J. (2002). Geochemistry of near-EPR seamounts: importance of source vs process and the origin of enriched mantle components. *Earth and Planetary Science Letters* **199**, 327–345.

Noble, R. H., Macintyre, R. M. & Brown, P. E. (1988). Age constraints on Atlantic evolution: timing of magmatic activity along the E Greenland continental margin. In: Morton, A. C. & Parson, L. M. (eds) *Early Tertiary Volcanism and the Opening of the NE Atlantic. Geological Society, London, Special Publications* **49**, 201–214.

Peate, D. W. & Stecher, O. (2002). Pb isotope evidence for contributions from different Iceland mantle components to Palaeogene East Greenland flood basalts. *Lithos*, in press.

Peate, D. W., Kokfelt, T. F., Hawkesworth, C. J., van Calsteren, P. W., Hergt, J. M. & Pearce, J. A. (2001). U-series isotope data on Lau Basin glasses: the role of subduction-related fluids during melt generation in back-arc basin basalts. *Journal of Petrology* **42**, 1449–1470.

Pedersen, A. K., Watt, M., Watt, W. S. & Larsen, L. M. (1997). Structure and stratigraphy of the Early Tertiary basalts of the Blosseville Kyst, East Greenland. *Journal of the Geological Society, London* **154**, 565–570.

Poreda, R. J., Schilling, J. G. & Craig, H. (1986). Helium and hydrogen isotopes in ocean ridge basalts north and south of Iceland. *Earth and Planetary Science Letters* **78**, 1–17.

Prestvik, T., Torske, T., Sundvoll, B. & Karlsson, H. (1999). Petrology of early Tertiary nephelinites off mid-Norway: additional evidence for an enriched endmember of the ancestral Iceland plume. *Lithos* **46**, 317–330.

Prestvik, T., Goldberg, S., Karlsson, H. & Gronvöld, K. (2001). Anomalous strontium and lead isotope signatures in the off-rift Öræfajökull central volcano in south-east Iceland: evidence for enriched endmember(s) of the Iceland mantle plume? *Earth and Planetary Science Letters* **190**, 211–220.

Salters, V. J. M. & White, W. M. (1998). Hf isotope constraints on mantle evolution. *Chemical Geology* **145**, 447–460.

Saunders, A. D., Fitton, J. G., Kerr, A. C., Norry, M. J. & Kent, R. W. (1997). The North Atlantic igneous province. In: Mahoney, J. J. & Coffin, M. F. (eds) *Large Igneous Provinces: Continental, Oceanic, and Planetary Flood Volcanism. Geophysical Monograph, American Geophysical Union* **100**, 45–94.

Saunders, A. D., Kempton, P. D., Fitton, J. G. & Larsen, L. M. (1999). Sr, Nd, and Pb isotopes and trace element geochemistry of basalts from the southeast Greenland margin. In: Larsen, H. C., Duncan, R. A., Allan, J. F. & Brooks, C. K. (eds) *Proceedings of the Ocean Drilling Program, Scientific Results, 163*. College Station, TX: Ocean Drilling Program, pp. 77–93.

Scarsi, P. (2000). Fractional extraction of helium by crushing of olivine and clinopyroxene phenocrysts: effects on the $^{3}He/^{4}He$ measured ratio. *Geochimica et Cosmochimica Acta* **64**, 3751–3762.

Schaefer, B. F., Parkinson, I. J. & Hawkesworth, C. J. (2000). Deep mantle plume osmium isotope signature from West Greenland Tertiary picrites. *Earth and Planetary Science Letters* **175**, 105–118.

Schilling, J.-G., Kingsley, R., Fontignie, D., Poreda, R. & Xue, S. (1999). Dispersion of the Jan Mayen and Iceland mantle plumes in the Arctic: a He–Pb–Nd–Sr isotope tracer study of basalts from the Kolbeinsey, Mohns and Knipovich Ridges. *Journal of Geophysical Research* **104**, 10543–10569.

Schoenberg, R., Nägler, T. F. & Kramers, J. D. (2000). Precise Os isotope ratio and Re–Os isotope dilution measurements down to the picogram level using multicollector inductively coupled plasma mass spectrometry. *International Journal of Mass Spectrometry* **197**, 85–94.

Shirey, S. B. & Walker, R. J. (1998). The Re–Os isotope system in cosmochemistry and high-temperature geochemistry. *Annual Review of Earth and Planetary Sciences* **26**, 423–500.

Skovgaard, A. C., Storey, M., Baker, J. A., Blusztajn, J. & Hart, S. R. (2001). Osmium–oxygen isotopic evidence for a recycled and strongly depleted component in the Iceland mantle plume. *Earth and Planetary Science Letters* **194**, 259–275.

Smit, Y., Parkinson, I. J., Peate, D. W., Cohen, A. S. & Hawkesworth, C. J. (2001). Os isotope and source characteristics of the Iceland plume. *Journal of Conference Abstracts* **6**(1), 452.

Smoliar, M. I., Walker, R. J. & Morgan, J. W. (1996). Re–Os ages of Group IIA, IIIA, IVA, and IVB iron meteorites. *Science* **271**, 1099–1102.

Stecher, O., Carlson, R. W. & Gunnarsson, B. (1999). Torfajökull: a radiogenic end-member of the Iceland Pb-isotopic array. *Earth and Planetary Science Letters* **165**, 117–127.

Storey, M., Duncan, R. A., Larsen, H. C., Pedersen, A. K., Waagstein, R., Larsen, L. M., Tegner, C. & Lesher, C. E. (1996). Impact and rapid flow of the Iceland plume beneath Greenland at 61 Ma. *EOS Transactions, American Geophysical Union* **77**, 839.

Storey, M., Duncan, R. A., Pedersen, A. K., Larsen, L. M. & Larsen, H. C. (1998). $^{40}Ar/^{39}Ar$ geochronology of the West Greenland Tertiary volcanic province. *Earth and Planetary Science Letters* **160**, 569–586.

Stuart, F. M., Ellam, R. M., Harrop, P. J., Fitton, J. G. & Bell, B. R. (2000). Constraints on mantle plumes from the helium isotopic composition of basalts from the British Tertiary Igneous Province. *Earth and Planetary Science Letters* **177**, 273–285.

Sun, S.-S. & Jahn, B. (1975). Lead and strontium isotopes in post-glacial basalts from Iceland. *Nature* **255**, 527–530.

Sun, S.-S. & McDonough, W. F. (1989). Chemical and isotopic systematics of oceanic basalts: implications for mantle composition and processes. In: Saunders, A. D. & Norry, M. J. (eds) *Magmatism in the Ocean Basins. Geological Society, London, Special Publications* **42**, 313–345.

Taylor, P. N., Kalsbeek, F. & Bridgwater, D. (1992). Discrepancies between neodymium, lead and strontium model ages from the Precambrian of southern East Greenland: evidence for a Proterozoic granulite-facies event affecting Archaean gneisses. *Chemical Geology (Isotope Geoscience Section)* **94**, 281–291.

Tegner, C. & Duncan, R. A. (1999). $^{40}Ar–^{39}Ar$ chronology for the oceanic history of the southeast Greenland rifted margin. In: Larsen, H. C., Duncan, R. A., Allan, J. F. & Brooks, C. K. (eds) *Proceedings of the Ocean Drilling Program, Scientific Results, 163*. College Station, TX: Ocean Drilling Program, pp. 53–62.

Tegner, C., Duncan, R. A., Bernstein, S., Brooks, C. K., Bird, D. K. & Storey, M. (1998*a*). $^{40}Ar/^{39}Ar$ geochronology of Tertiary mafic intrusions along the East Greenland rifted margin: relation to flood basalts and the Iceland hotspot track. *Earth and Planetary Science Letters* **156**, 75–88.

Tegner, C., Lesher, C. E., Larsen, L. M. & Watt, W. S. (1998*b*). Evidence from the rare-earth-element record of mantle melting for cooling of the Tertiary Iceland plume. *Nature* **395**, 591–594.

Thirlwall, M. F. (1997). Pb isotopic and elemental evidence for OIB derivation from young HIMU mantle. *Chemical Geology* **139**, 51–74.

Thirlwall, M. F. (2000). Inter-laboratory and other errors in Pb isotope analyses investigated using a $^{207}Pb–^{204}Pb$ double spike. *Chemical Geology* **163**, 299–322.

Thirlwall, M. F., Upton, B. G. J. & Jenkins, C. (1994). Interaction between continental lithosphere and the Iceland plume: Sr–Nd–Pb isotope geochemistry of Tertiary basalts, NE Greenland. *Journal of Petrology* **35**, 839–879.

Torsvik, T. H., Mosar, J. & Eide, E. A. (2001). Cretaceous–Tertiary geodynamics: a North Atlantic exercise. *Geophysical Journal International* **146**, 850–866.

Trønnes, R. G., Planke, S., Sundvoll, B. A. & Imsland, P. (1999). Recent volcanic rocks from Jan Mayen: low-degree melt fractions of enriched northeast Atlantic mantle. *Journal of Geophysical Research* **104**, 7153–7168.

Vervoort, J. D., Patchett, P. J., Blichert-Toft, J. & Albarède, F. (1999). Relationships between Lu–Hf and Sm–Nd systems in the global sedimentary system. *Earth and Planetary Science Letters* **168**, 79–99.

Wager, L. R. (1947). Geological investigations in East Greenland: part IV, The stratigraphy and tectonics of Knud Rasmussen Land and the Kangerdlugssuaq region. *Meddelelser om Grønland* **134**, 2–64.

Waight, T. E., Baker, J. A. & Peate, D. W. (2002*a*). Sr isotope measurements by double-focusing MC-ICPMS: techniques, observations and pitfalls. *International Journal of Mass Spectrometry*, in press.

Waight, T. E., Baker, J. A. & Willigers, B. (2002*b*). Rb isotope dilution analyses by MC-ICP-MS using Zr to correct for mass fractionation: towards improved Rb–Sr geochronology. *Chemical Geology* **186**, 99–116.

Weaver, B. (1991). The origin of ocean island basalt end-member compositions: trace element and isotopic constraints. *Earth and Planetary Science Letters* **104**, 381–397.